Industrial & Engineering Chemistry Research

Electronic Supporting Information

Towards development of a universal CP-PC-SAFT-based modeling framework for predicting thermophysical properties at reservoir conditions: inclusion of surface tensions.

José Matías Garrido[a], Ilya Polishuk[b,*]

[a]Departamento de Ingeniería Química, Universidad de Concepción, Concepción, Chile.

[b]Department of Chemical Engineering & Biotechnology, Ariel University, 40700, Ariel, Israel.

[*]Corresponding author. E-mail address: polishuk@ariel.ac.il

Table S1. Parameter solutions for the compounds considered in this study.

Compound	m	ε/k_B [K]	σ [Å]	ε^{AB}/k_b [K] *	κ^{AB} *	$10^{19} \times \chi$[J m^5/mol^2]
water	1.61753	72.816	2.42813	2070.0	0.2280	0.34094
ethanol	2.78275	167.346	3.03211	2650.0	0.0787	0.68295
carbon dioxide	2.03351	163.491	2.81786	-	-	0.26878
nitrogen	0.99880	94.3513	3.61590	-	-	0.11819
methane	1.00082	142.508	3.74760	-	-	0.19808
n - ethane	1.56358	185.392	3.57406	-	-	0.48251
n - propane	2.41440	184.368	3.39176	-	-	0.80323
n - butane	2.48262	209.446	3.65040	-	-	1.45833
n - pentane	3.06424	212.528	3.62421	-	-	2.07941
n - hexane	3.51081	218.238	3.65575	-	-	3.05047
n - heptane	4.07032	220.494	3.63515	-	-	3.81138
n - octane	4.45475	225.287	3.67868	-	-	4.85782
n - decane	5.27013	232.262	3.72188	-	-	7.61263
n - tetradecane	7.04293	240.579	3.75151	-	-	14.2130
n - hexadecane	7.58776	246.366	3.81901	-	-	18.9565
n - octadecane	7.89201	252.131	3.91545	-	-	25.1920
toluene	3.70532	249.535	3.40065	-	-	2.33917

* - According to the proposed approach, ε^{AB}/k_b and κ^{AB} are the fitted parameters of associated compounds. The rest of the parameters are solved.

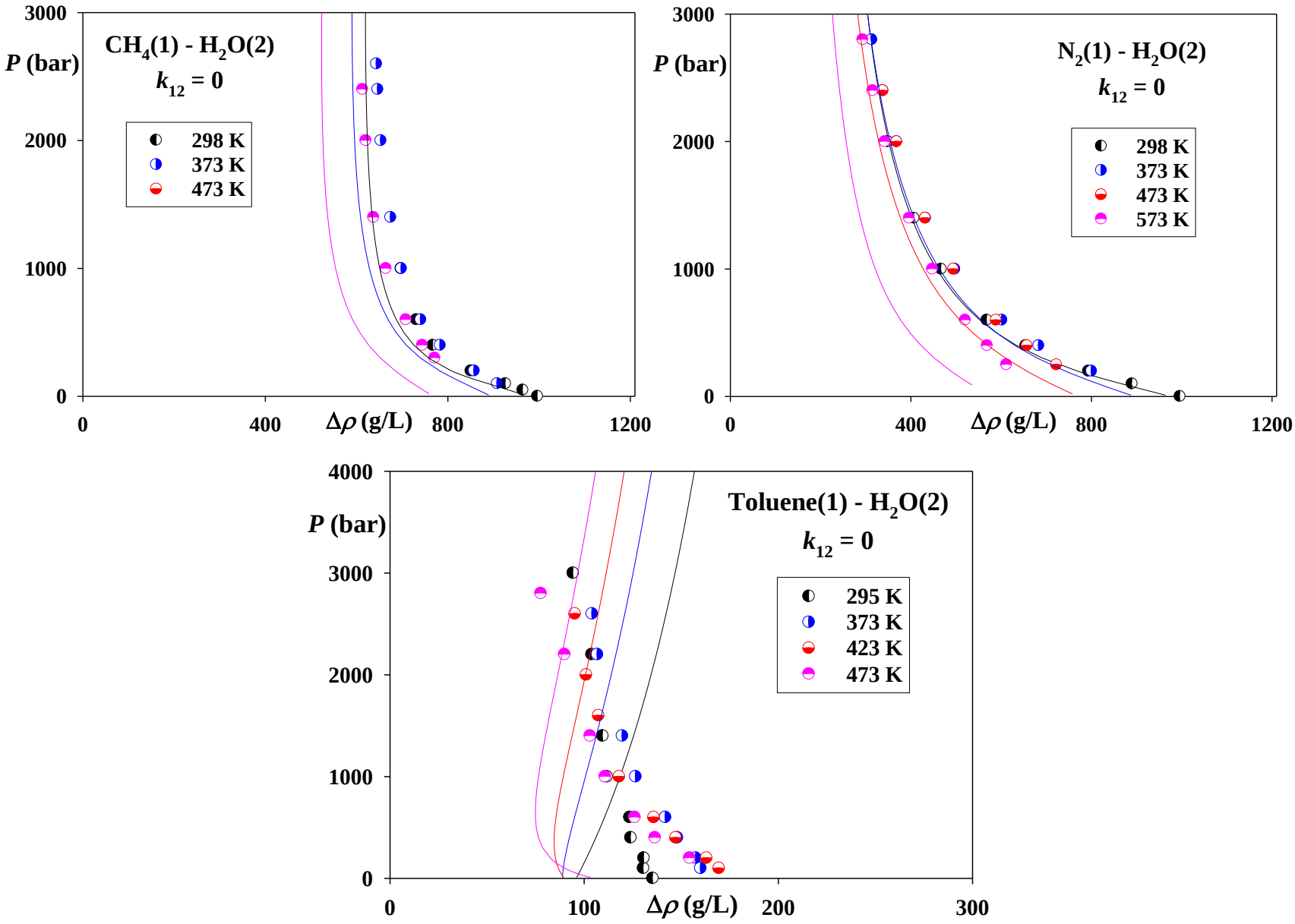

Figure S1. Differences between the equilibria phase densities in aqueous systems. Points – experimental data[1]. Lines – predictions of CP-PC-SAFT.

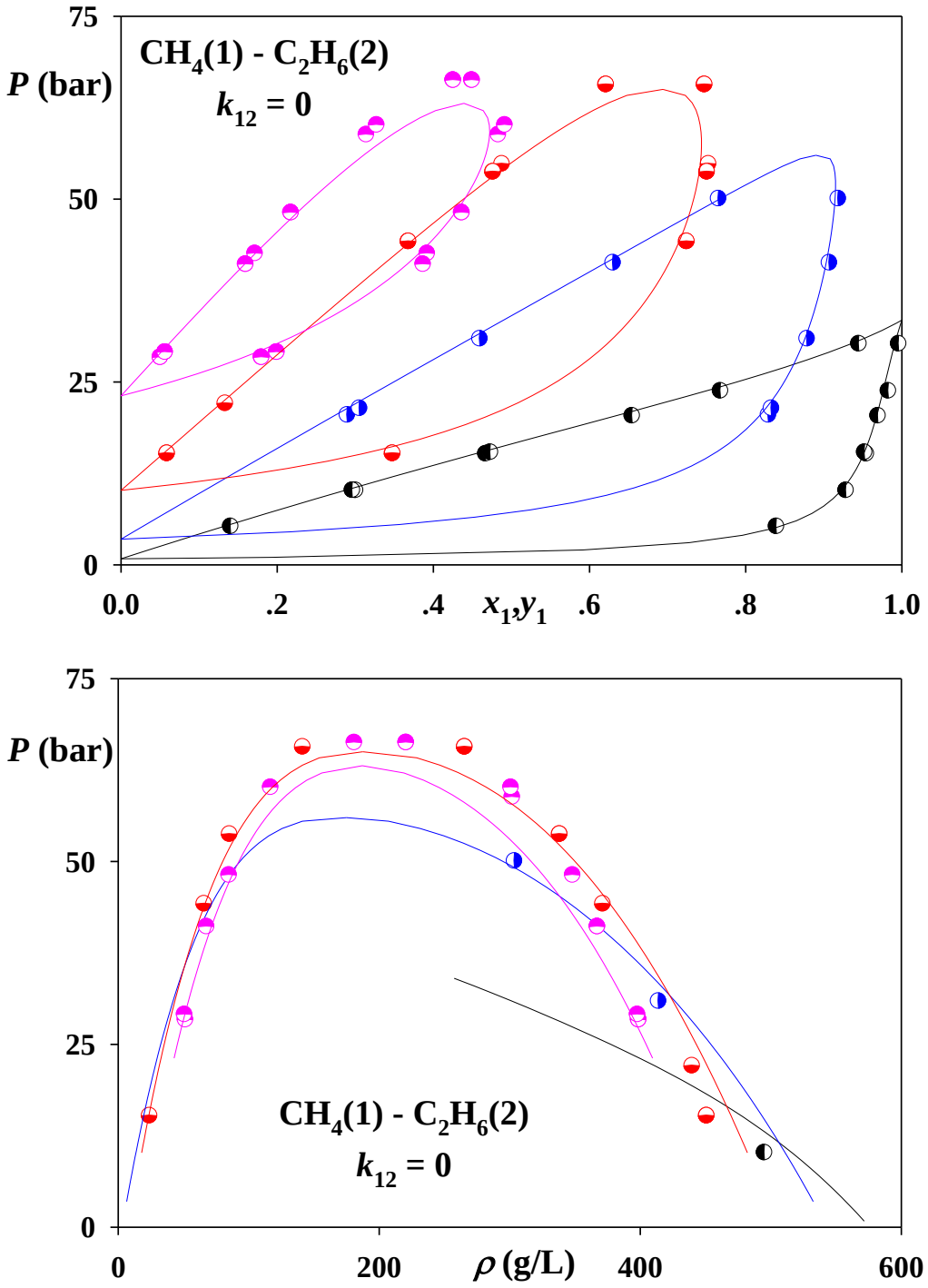

Figure S2. VLE and saturated phase densities of methane(1) – ethane(2). Experimental data[2,3]:

◑ – 180 K, ◐ – 210 K, ◓ – 240 K, ◒ – 270 K. Lines – predictions of CP-PC-SAFT.

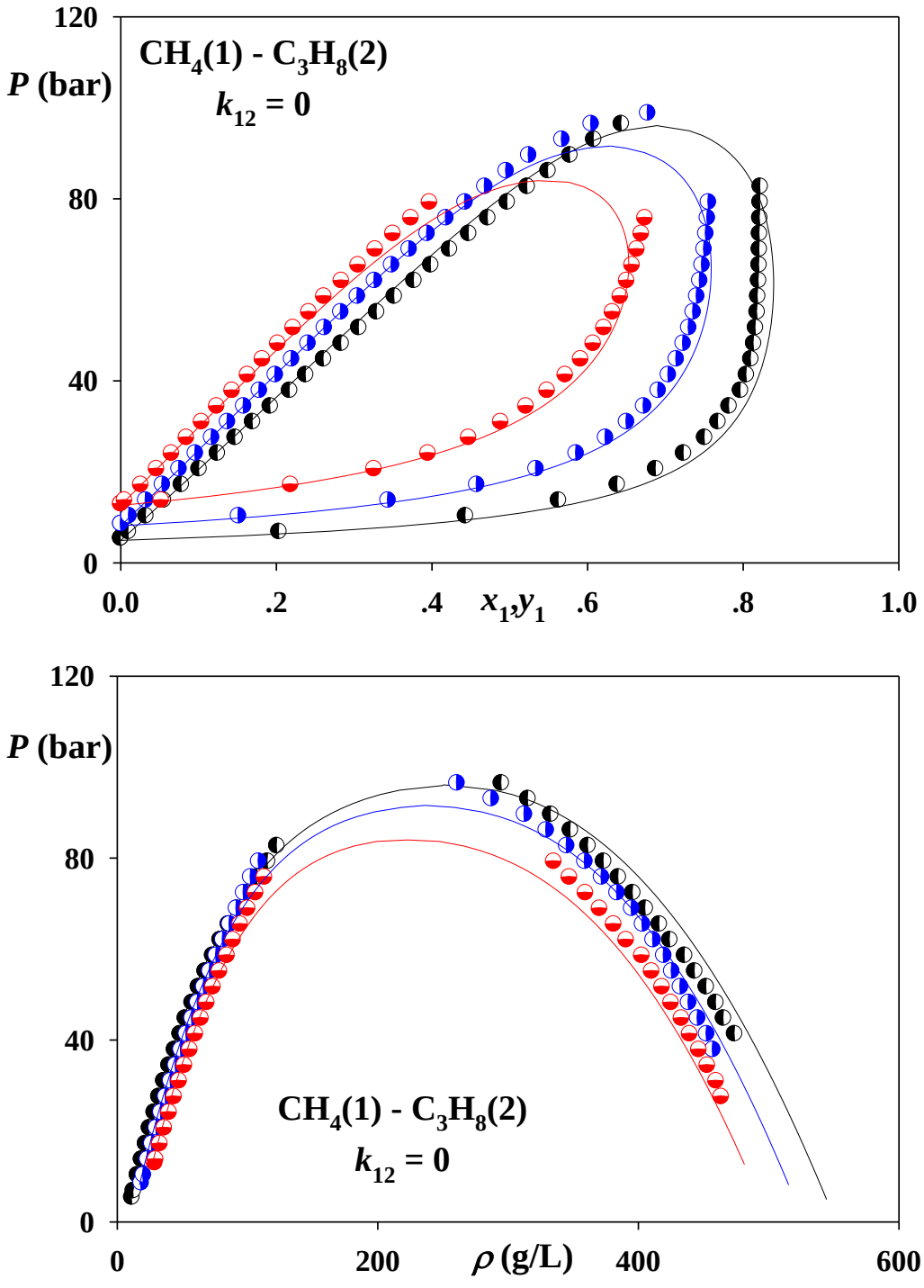

Figure S3. VLE and saturated phase densities of methane(1) – propane(2). Experimental data[4]:

◑ – 277.59 K, ◐ – 294.26 K, ◓ – 310.93 K. Lines – predictions of CP-PC-SAFT.

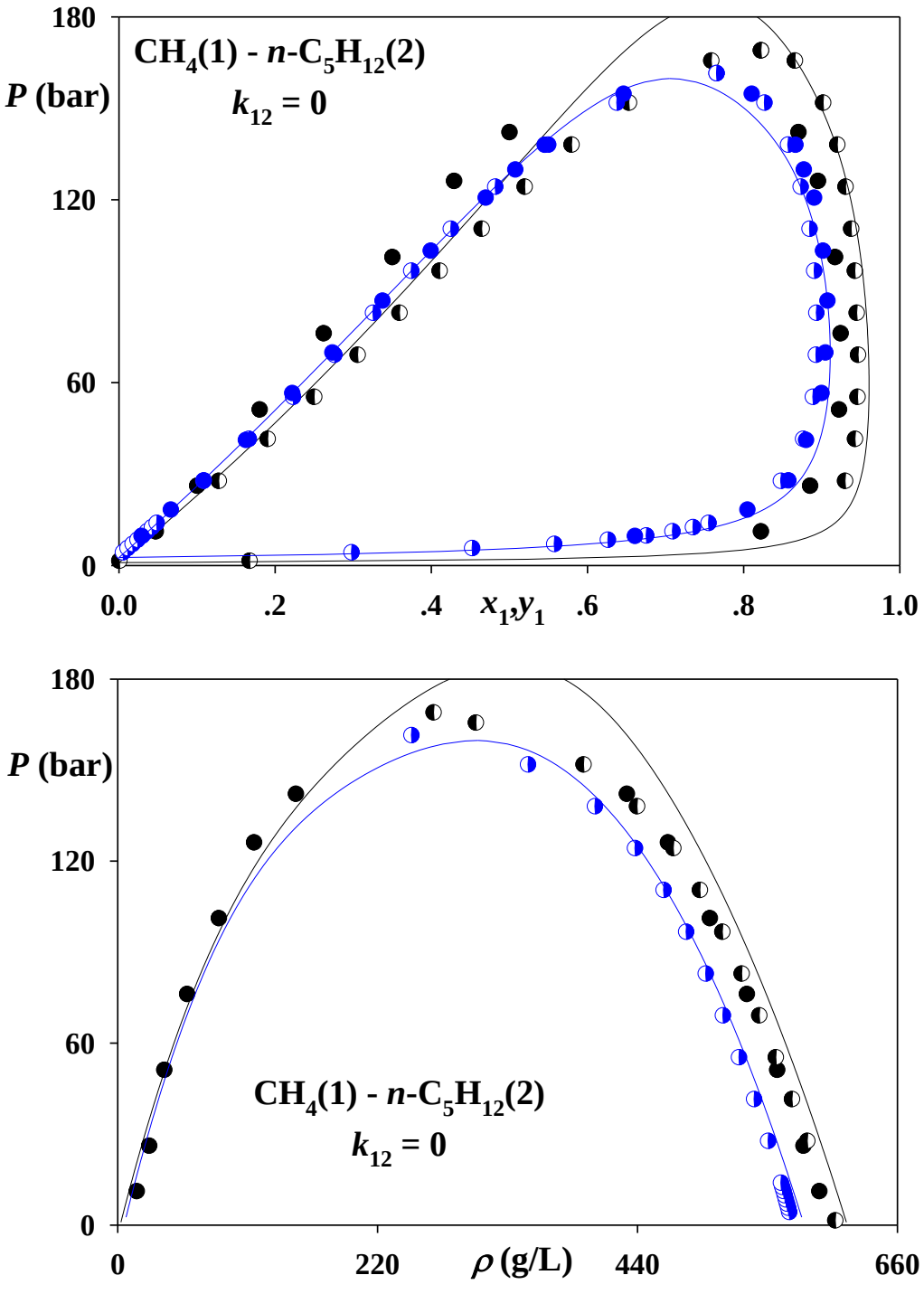

Figure S4. VLE and saturated phase densities of methane(1) – *n*-pentane(2). Experimental data:

◑ – 310.93 K, ◐ – 344.26 K[5]; ● – 313.15 K[6]; ● – 344.45 K[7].

Lines – predictions of CP-PC-SAFT.

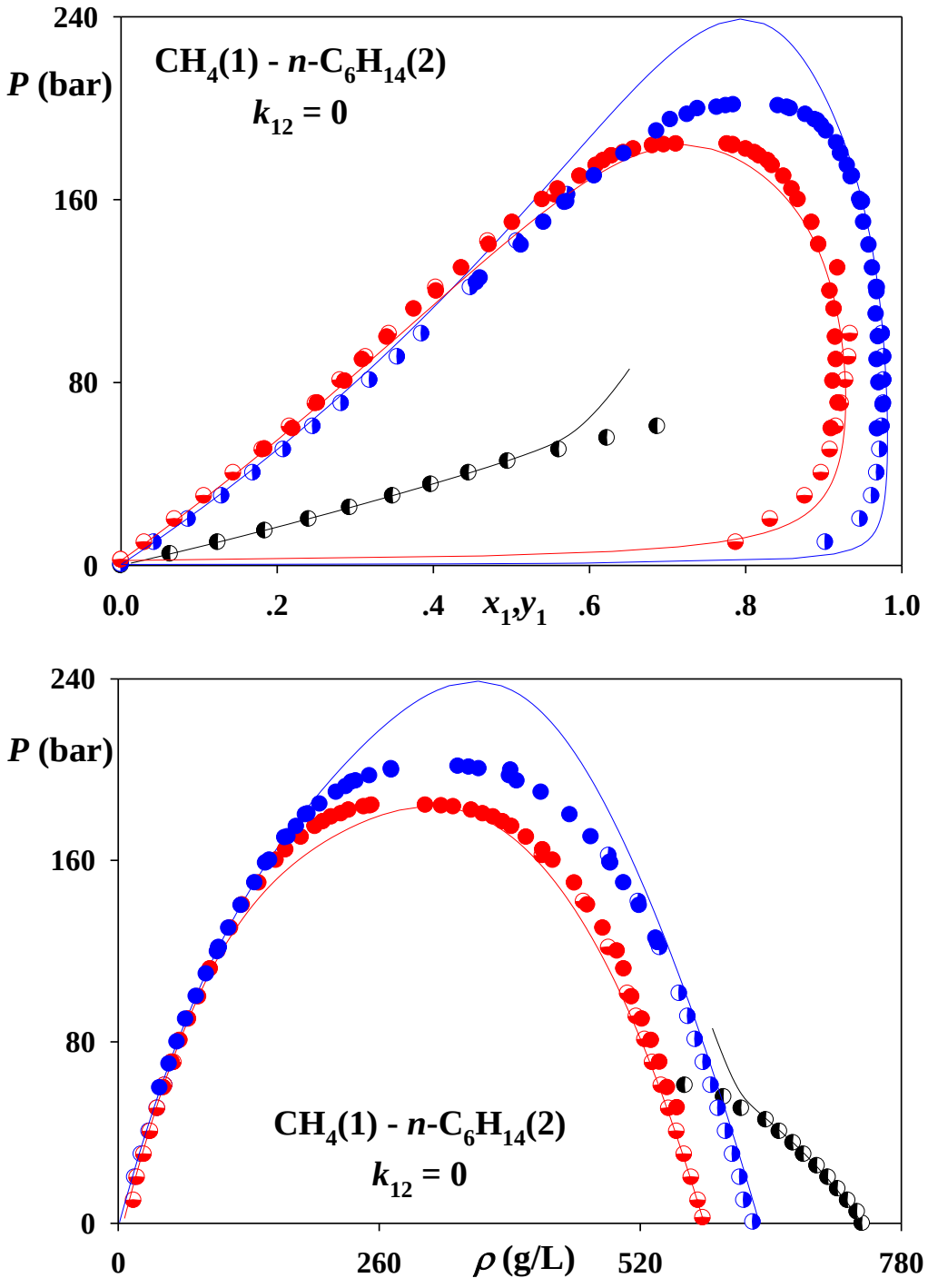

Figure S5. VLE and saturated phase densities of methane(1) – *n*-hexane(2). Experimental data:

◑ – 198.15 K, ◐ – 323.15 K, ◓ – 373.15 K[8]; ● – 323 K[6]; ● – 373 K[9].

Lines – predictions of CP-PC-SAFT.

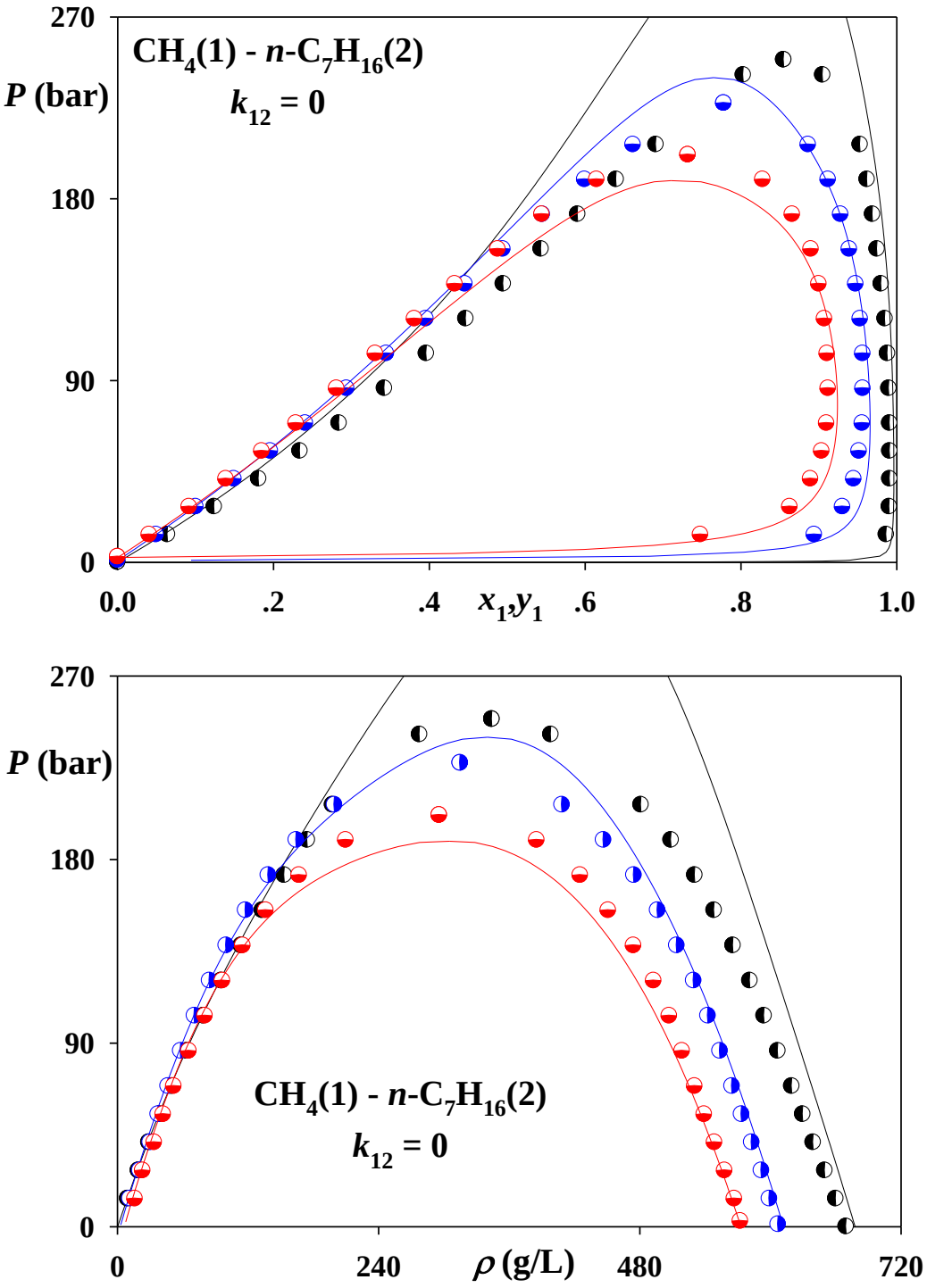

Figure S6. VLE and saturated phase densities of methane(1) – *n*-heptane(2). Experimental data[10]: ◑ – 310.93 K, ◐ – 377.59 K, ◓ – 410.93 K. Lines – predictions of CP-PC-SAFT.

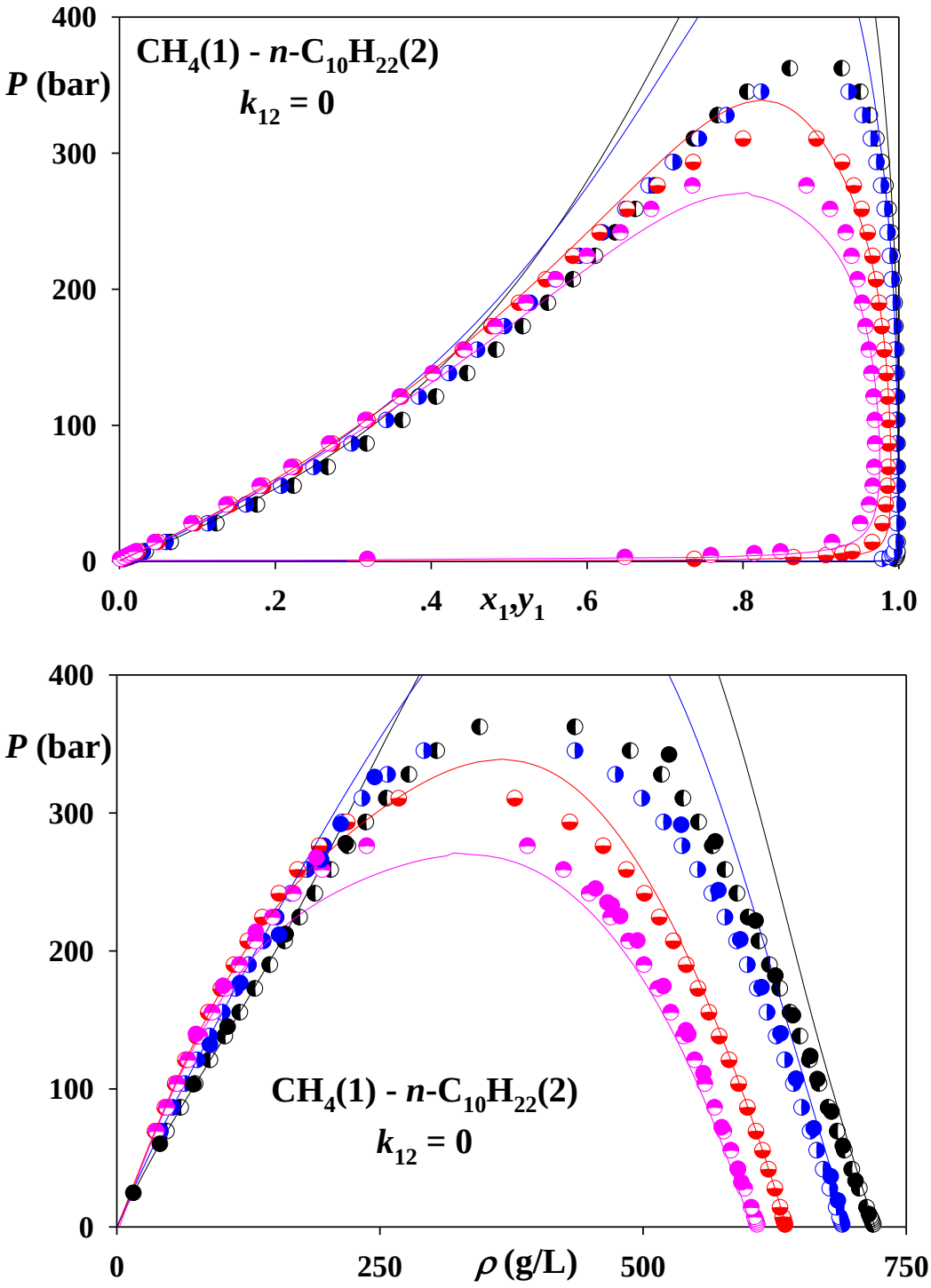

Figure S7. VLE and saturated phase densities of methane(1) – *n*-decane(2). Experimental data:

◑ – 310.93 K, ◐ – 344.26 K, ◓ – 410.93 K, ◒ – 444.26 K[11].

● – 313.1 K, ● – 343.3 K, ● – 442.8 K[12]. Lines – predictions of CP-PC-SAFT.

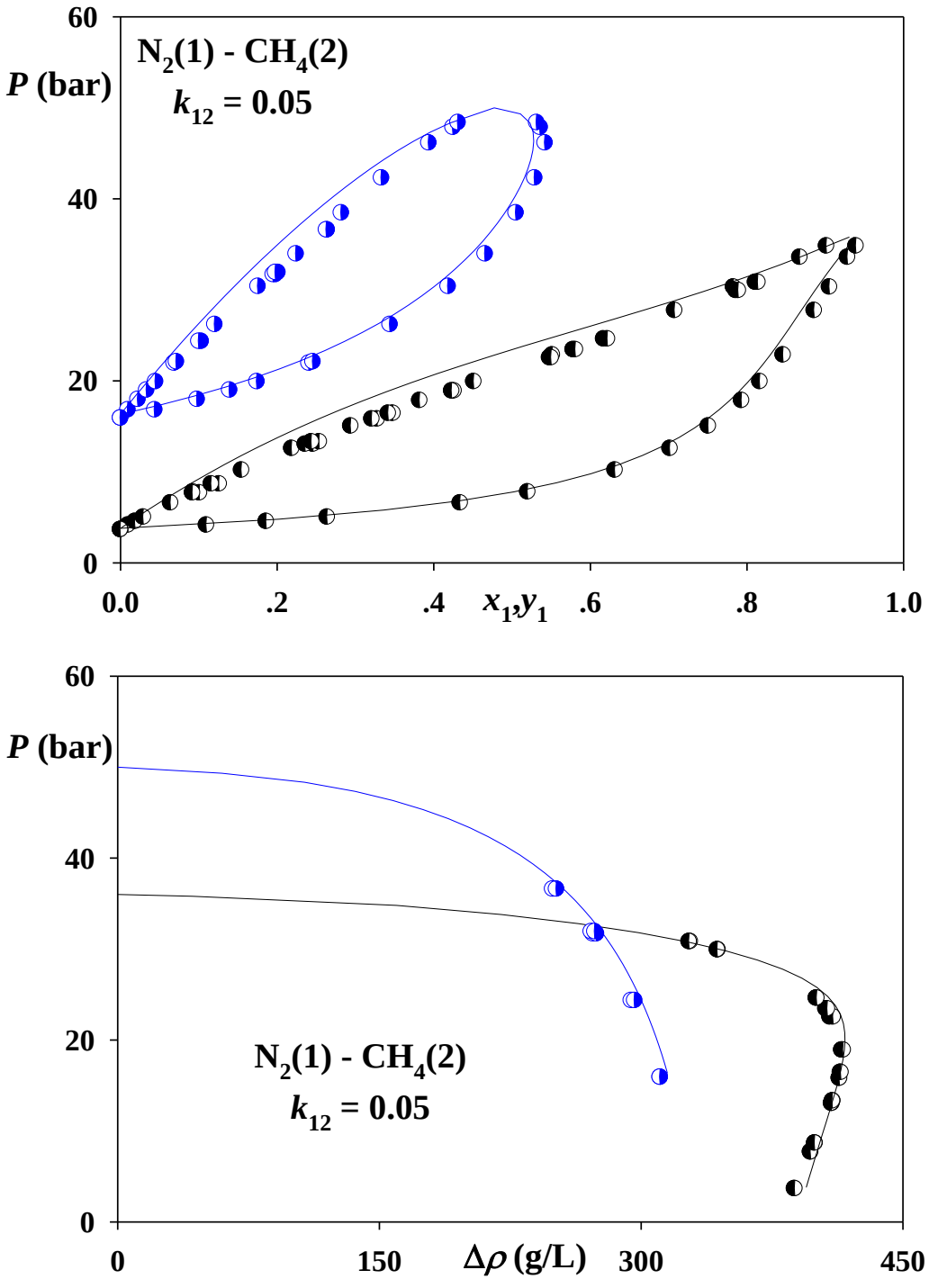

Figure S8. VLE and saturated phase densities of nitrogen(1) – methane(2). Experimental data[13,14]:

◑ – 130 K, ◐ – 160 K. Lines – results of CP-PC-SAFT.

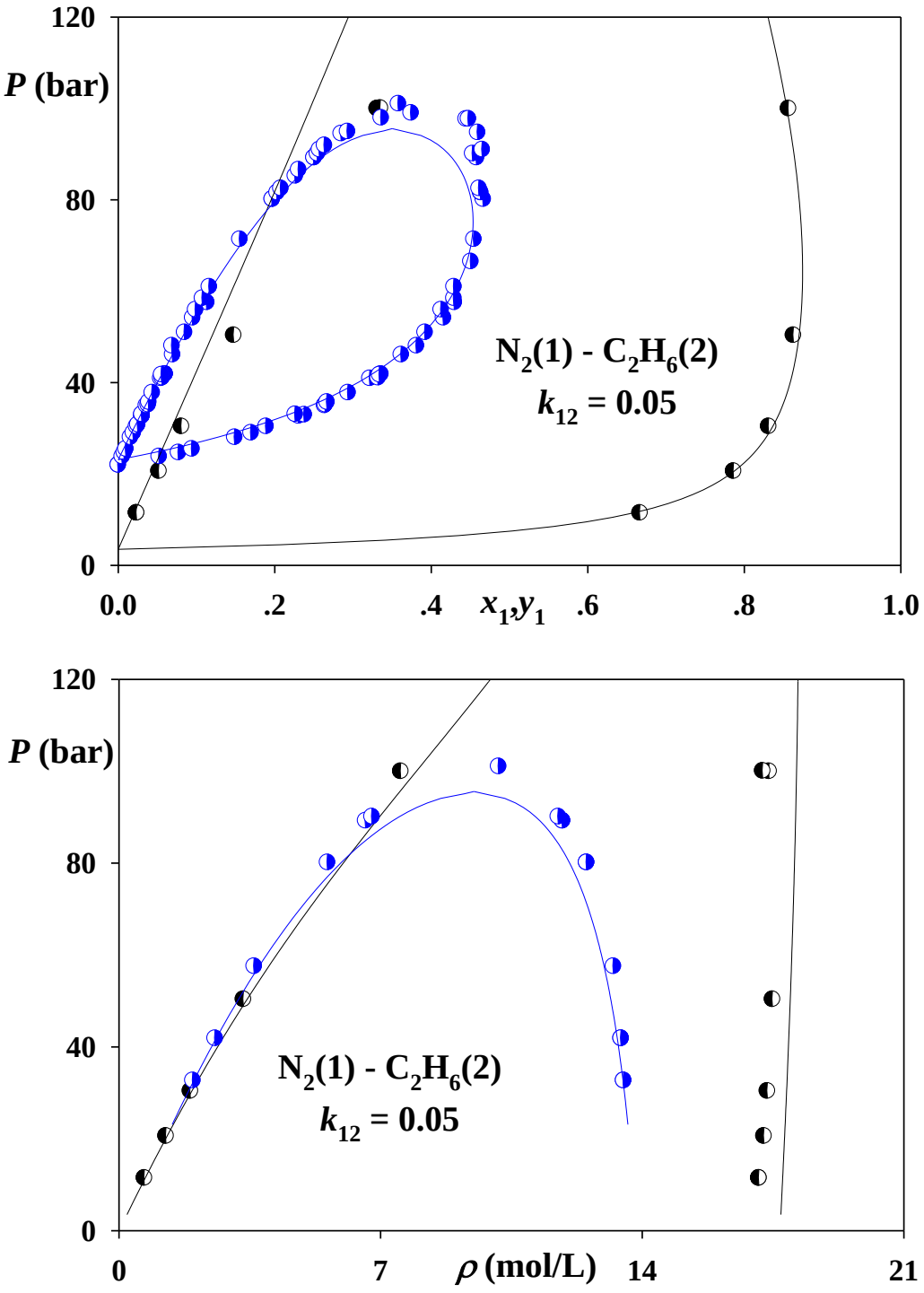

Figure S9. VLE and saturated phase densities of nitrogen(1) – ethane(2). Experimental data[2,3,15]:

◑ – 130 K, ◐ – 160 K. Lines – results of CP-PC-SAFT.

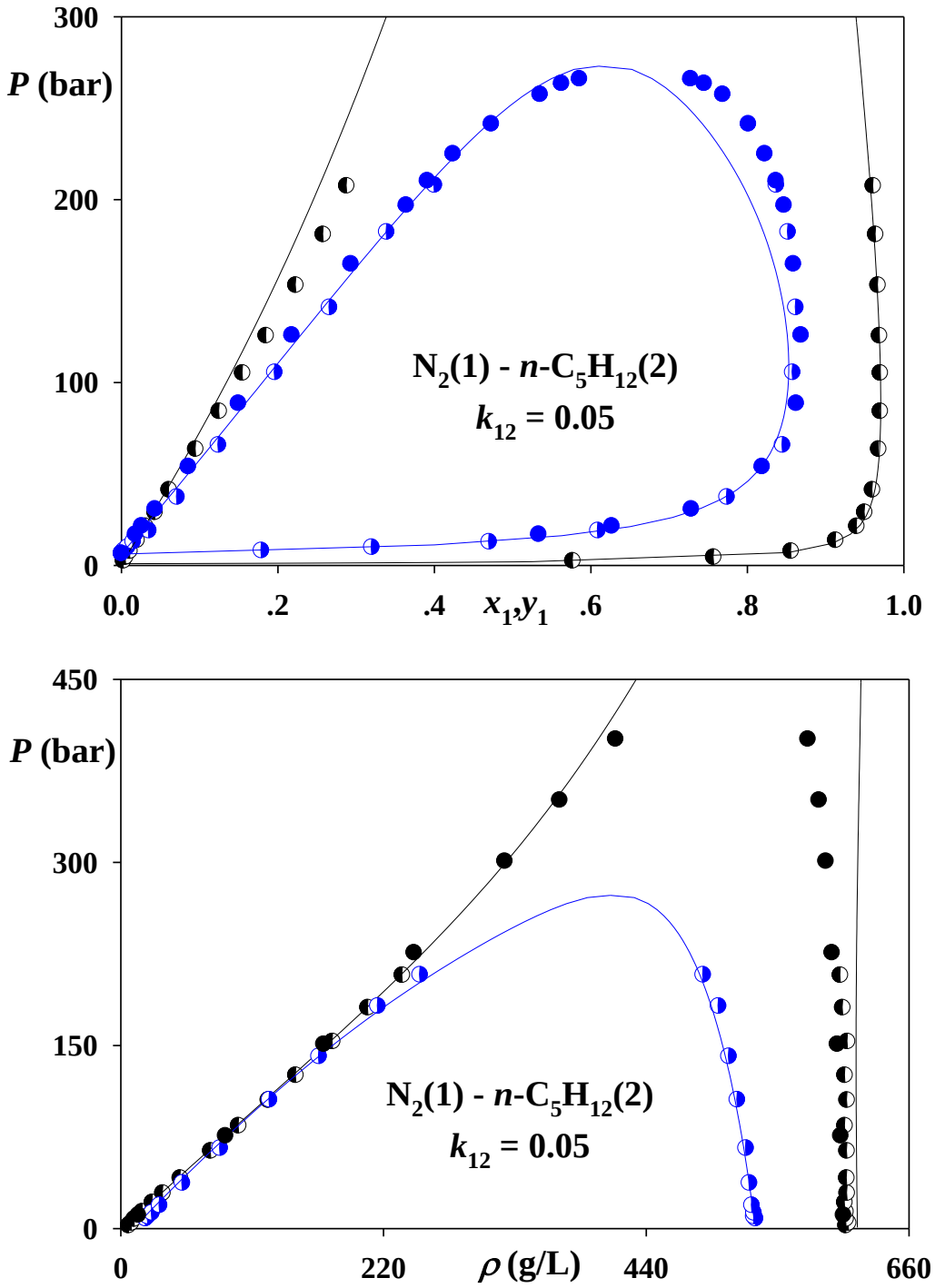

Figure S10. VLE and saturated phase densities of nitrogen(1) – *n*-pentane(2). Experimental data:

◑ – 310.73 K, ◐ – 377.59 K[16]; ● – 313.15 K (17); ● – 377.9 K[18].

Lines – results of CP-PC-SAFT.

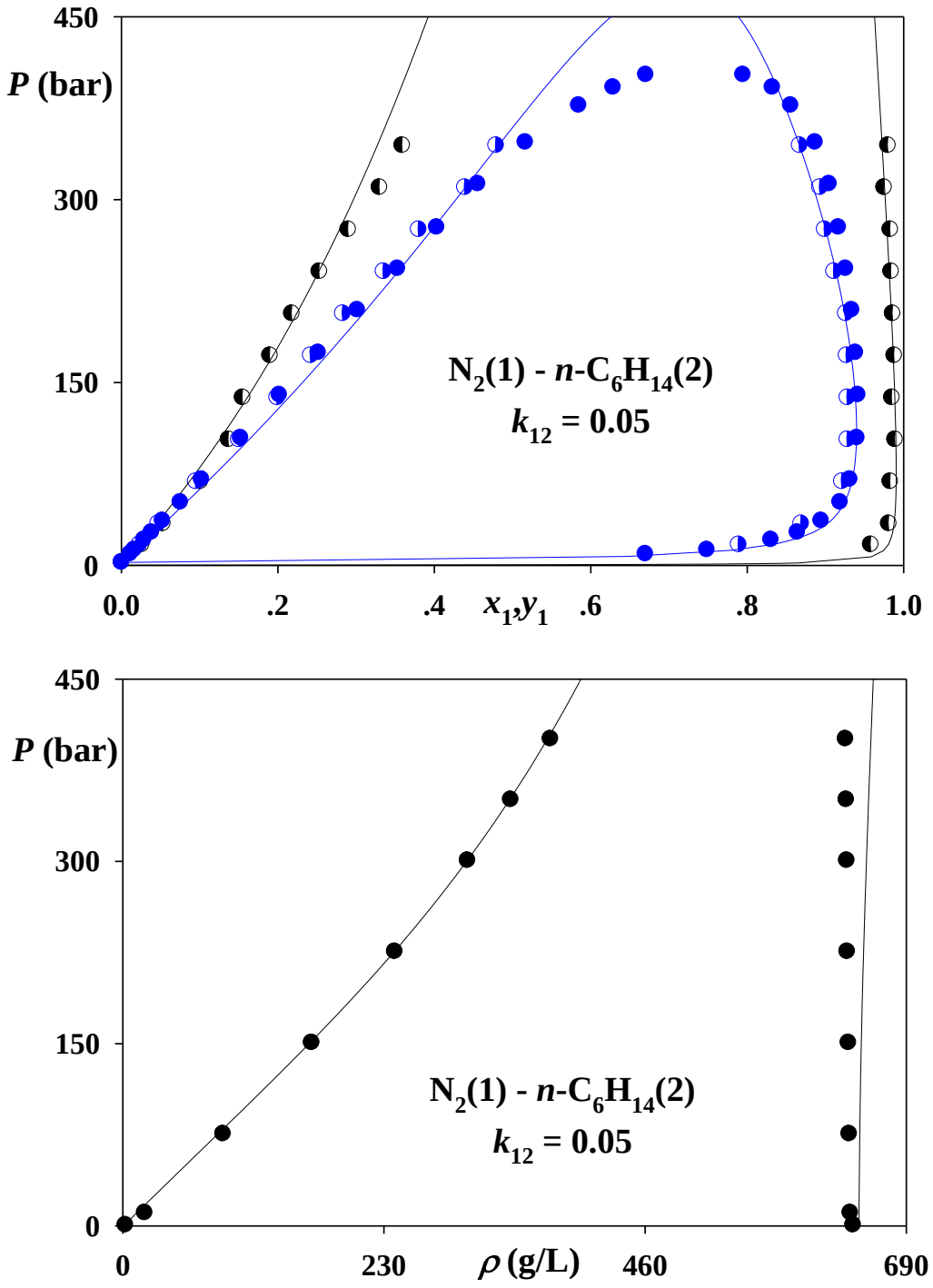

Figure S11. VLE and saturated phase densities of nitrogen(1) – *n*-hexane(2). Experimental data:

◑ – 310.93 K, ◐ – 377.55 K[19]; ● – 313.15 K[17]; ● – 377.9 K[20].

Lines – results of CP-PC-SAFT.

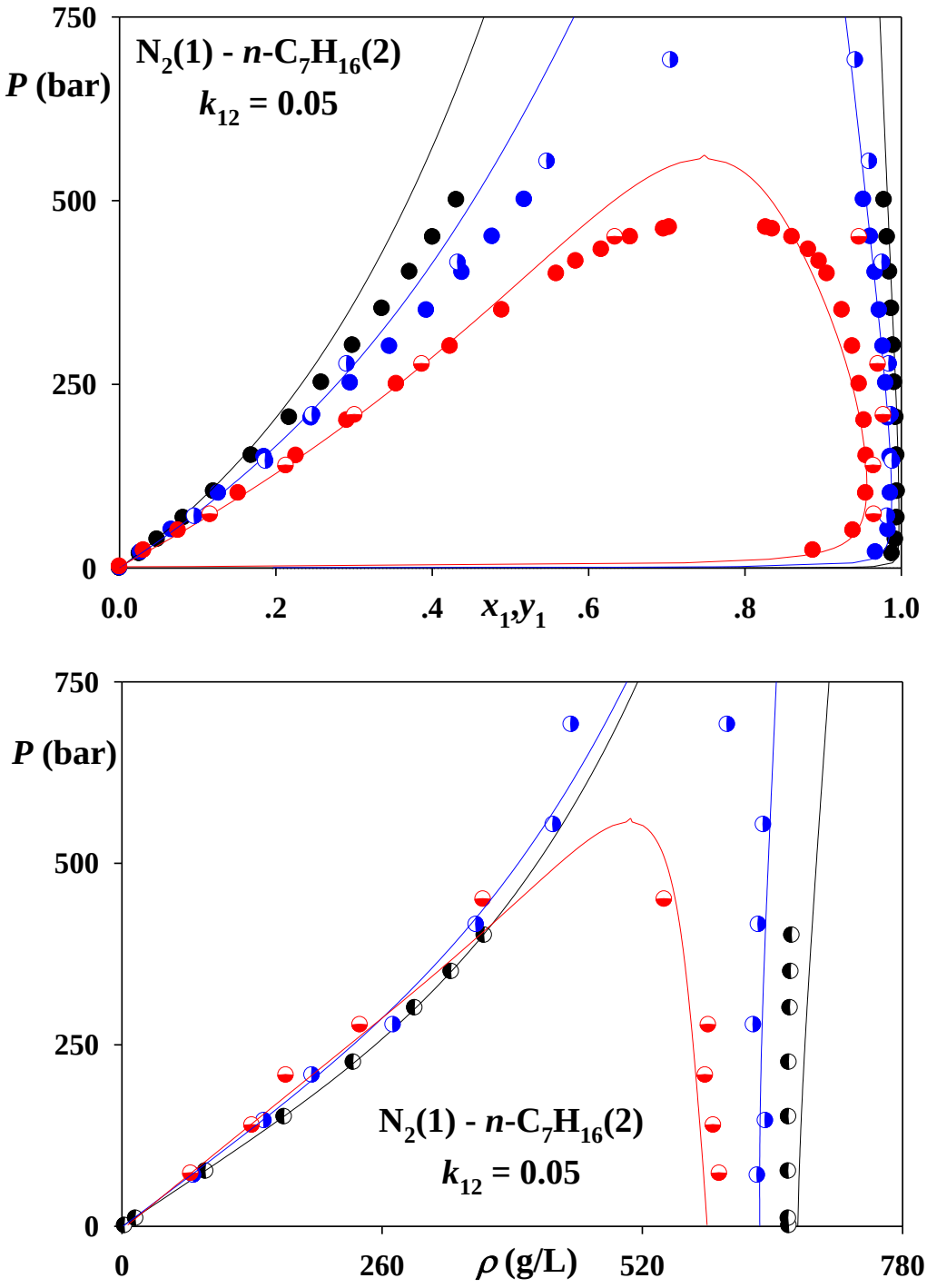

Figure S12. VLE and saturated phase densities of nitrogen(1) – *n*-heptane(2). Experimental data:

◑ – 313.15 K[17]; ● – 313.6 K, ● – 353.4 K, ● – 400.4 K[21]; ◐ – 352.59 K, ◓ – 399.82 K[22];

Lines – results of CP-PC-SAFT.

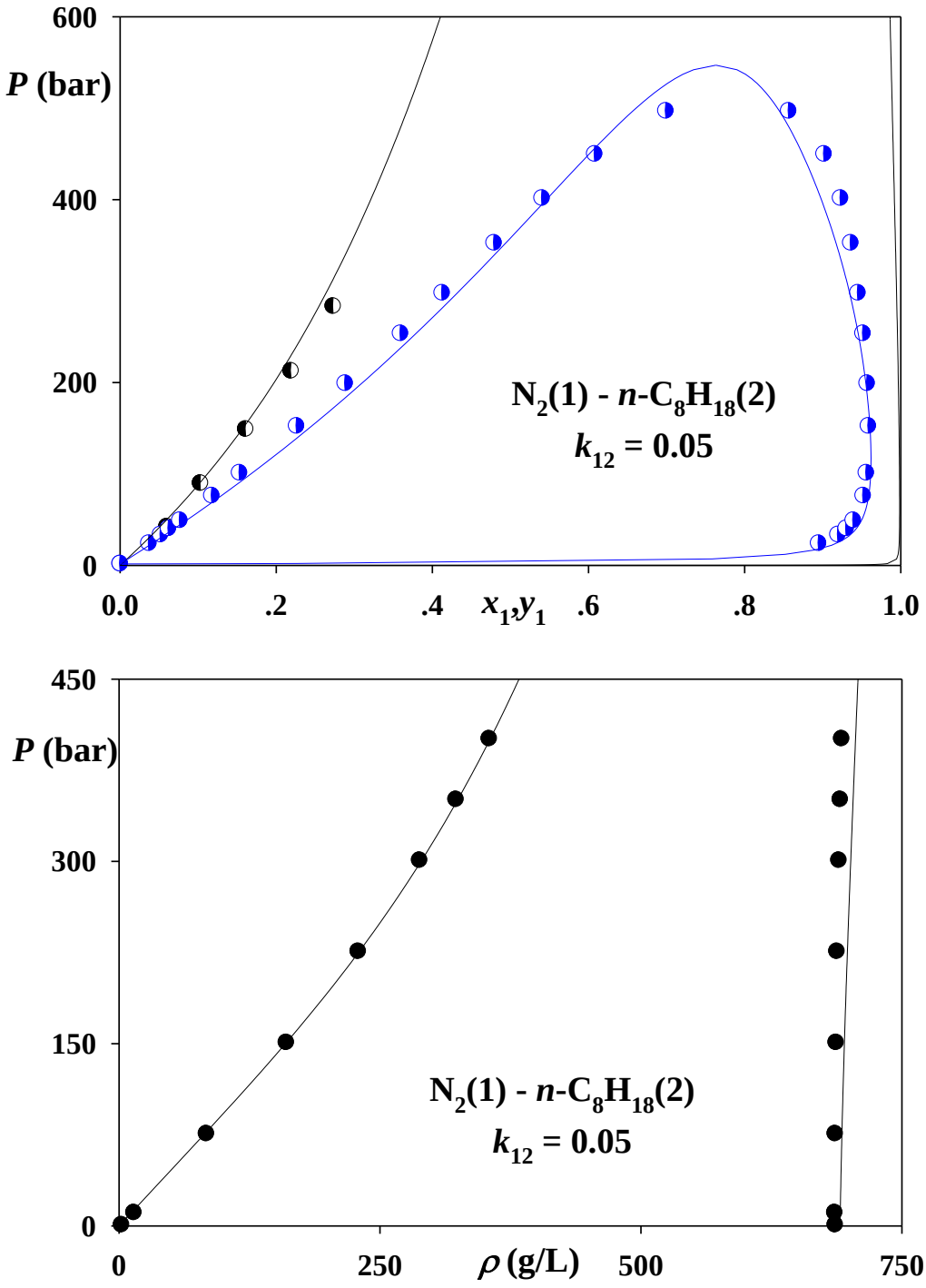

Figure S13. VLE and saturated phase densities of nitrogen(1) – *n*-octane(2). Experimental data:

● – 313.15 K[17]; ◑ – 322 K[23] ◐ – 424 K[24]; Lines – results of CP-PC-SAFT.

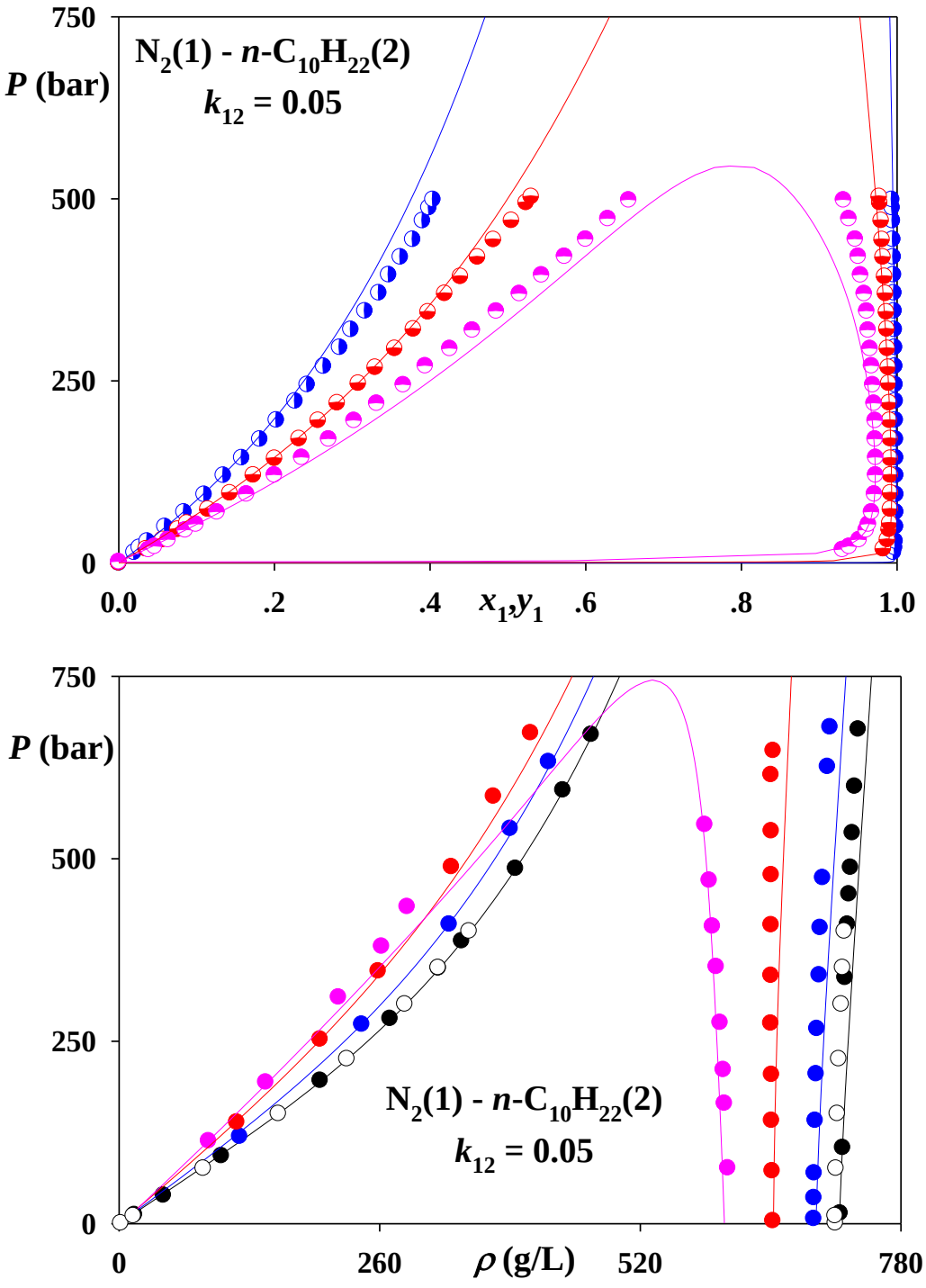

Figure S14. VLE and saturated phase densities of nitrogen(1) – *n*-decane(2). Experimental data: ○ – 313.15 K[17]; ◐ – 344.6 K, ◓ – 410.9 K, ◒ – 463.7 K[25]; ● – 313.2 K, ● – 343.5 K, ● – 393.3 K, ● – 443.2 K[12]; Lines – results of CP-PC-SAFT.

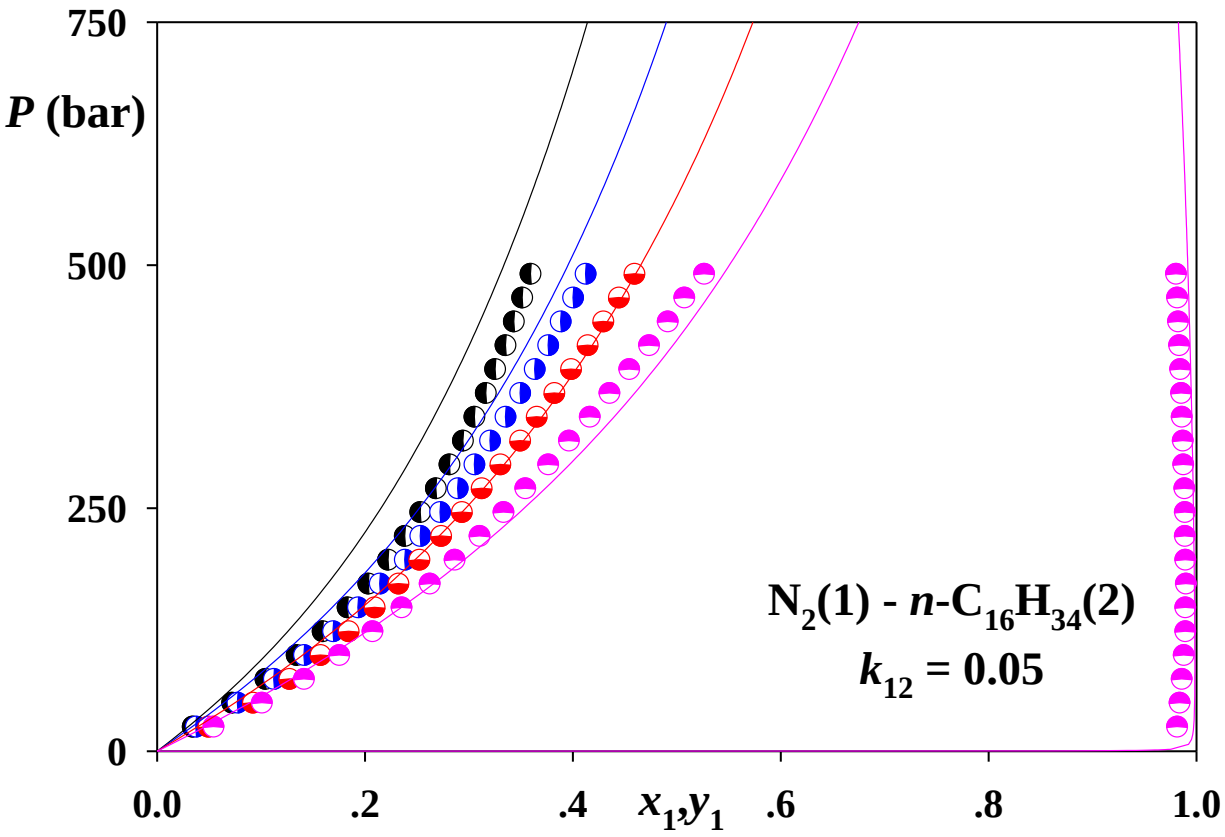

Figure S15. VLE of nitrogen(1) – *n*-hexadecane(2). Experimental data:

◑ – 323.15 K, ◐ – 373.15 K, ◓ – 423.15 K ◒ – 473.15 K[26]; Lines – results of CP-PC-SAFT.

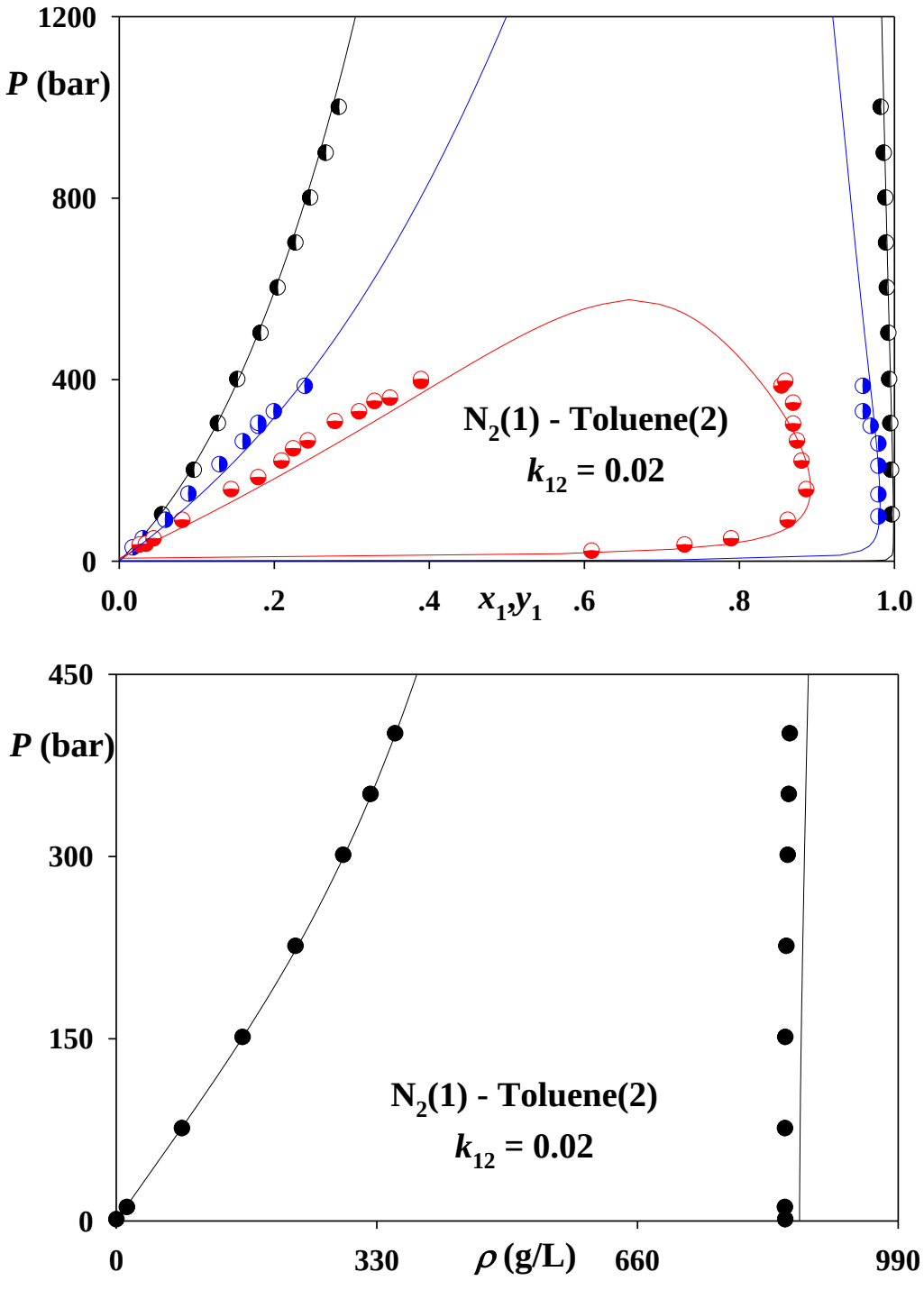

Figure S16. VLE and saturated phase densities of nitrogen(1) – toluene(2). Experimental data:

● – 313.15 K[16]; ◑ – 313.2 K, ◐ – 391.5 K, ◓ – 472.6 K[27];

Lines – results of CP-PC-SAFT.

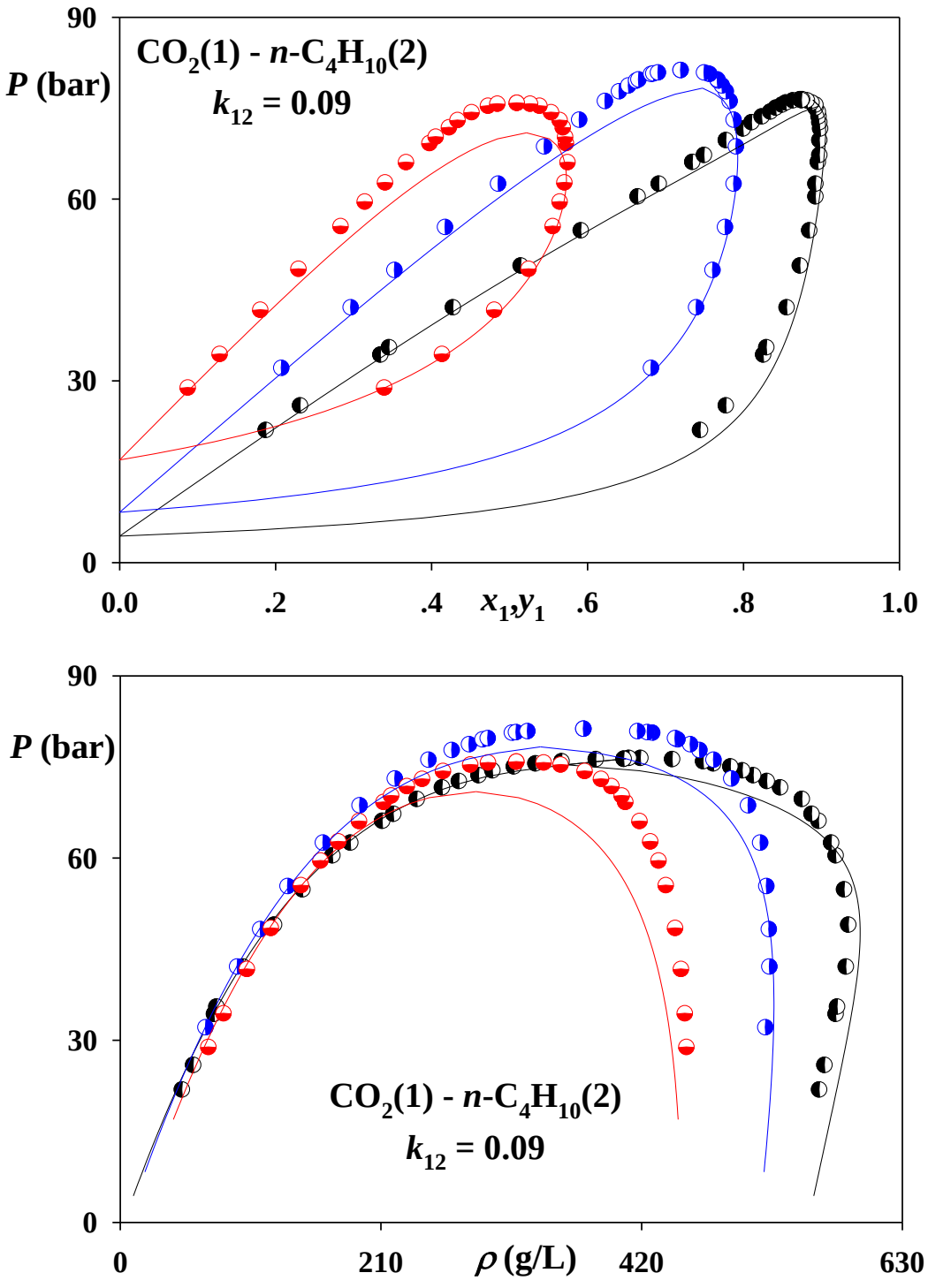

Figure S17. VLE and saturated phase densities of carbon dioxide(1) – *n*-butane(2).

Experimental data[28]: ◑ – 319.3 K, ◐ – 344.3 K, ◓ – 377.6 K. Lines – results of CP-PC-SAFT.

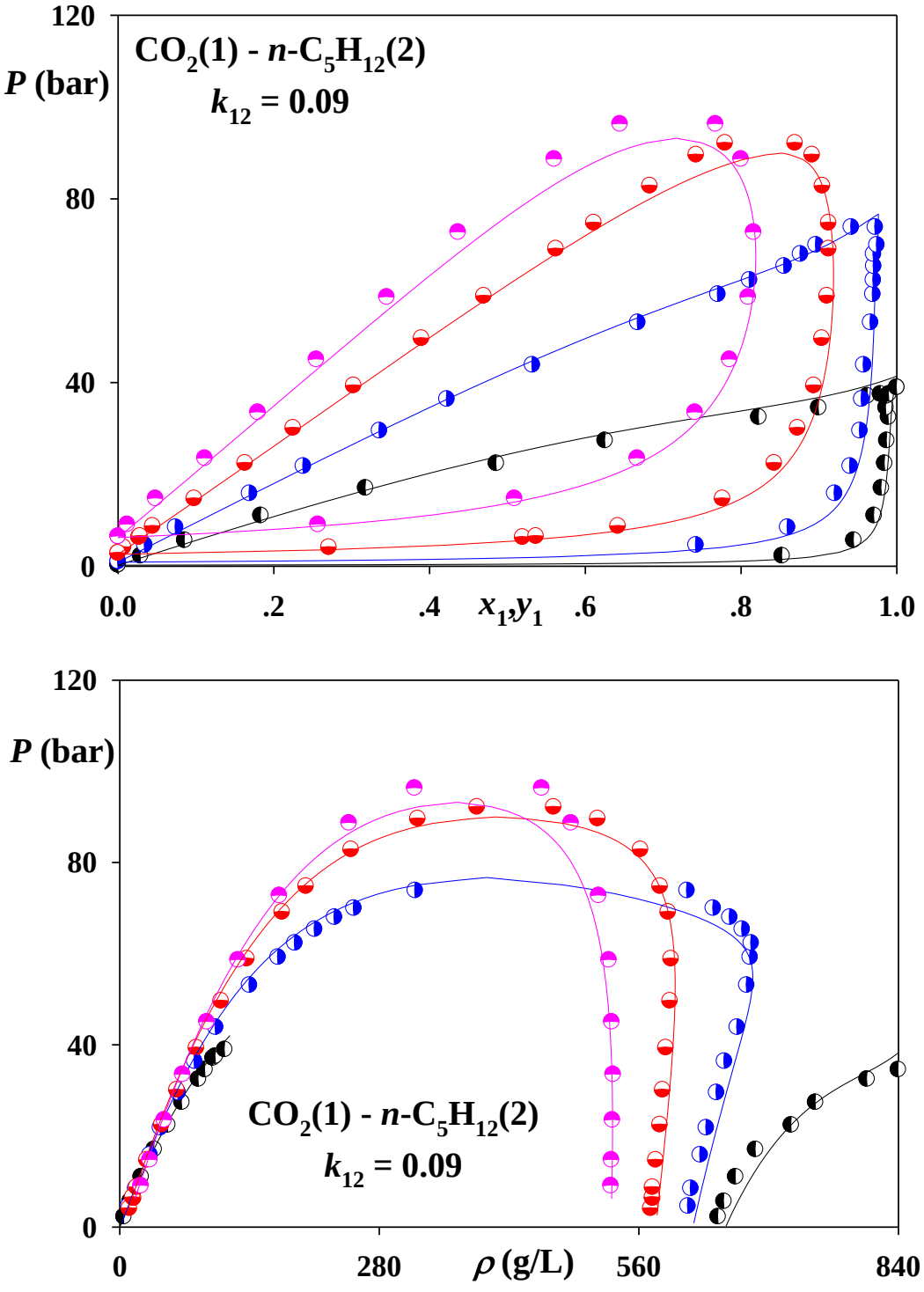

Figure S18. VLE and saturated phase densities of carbon dioxide(1) – *n*-pentane(2). Experimental data[29]: ◑ – 277.59 K, ◐ – 310.93 K, ◓ – 343.71 K, ◒ – 377.59 K. Lines – results of CP-PC-SAFT.

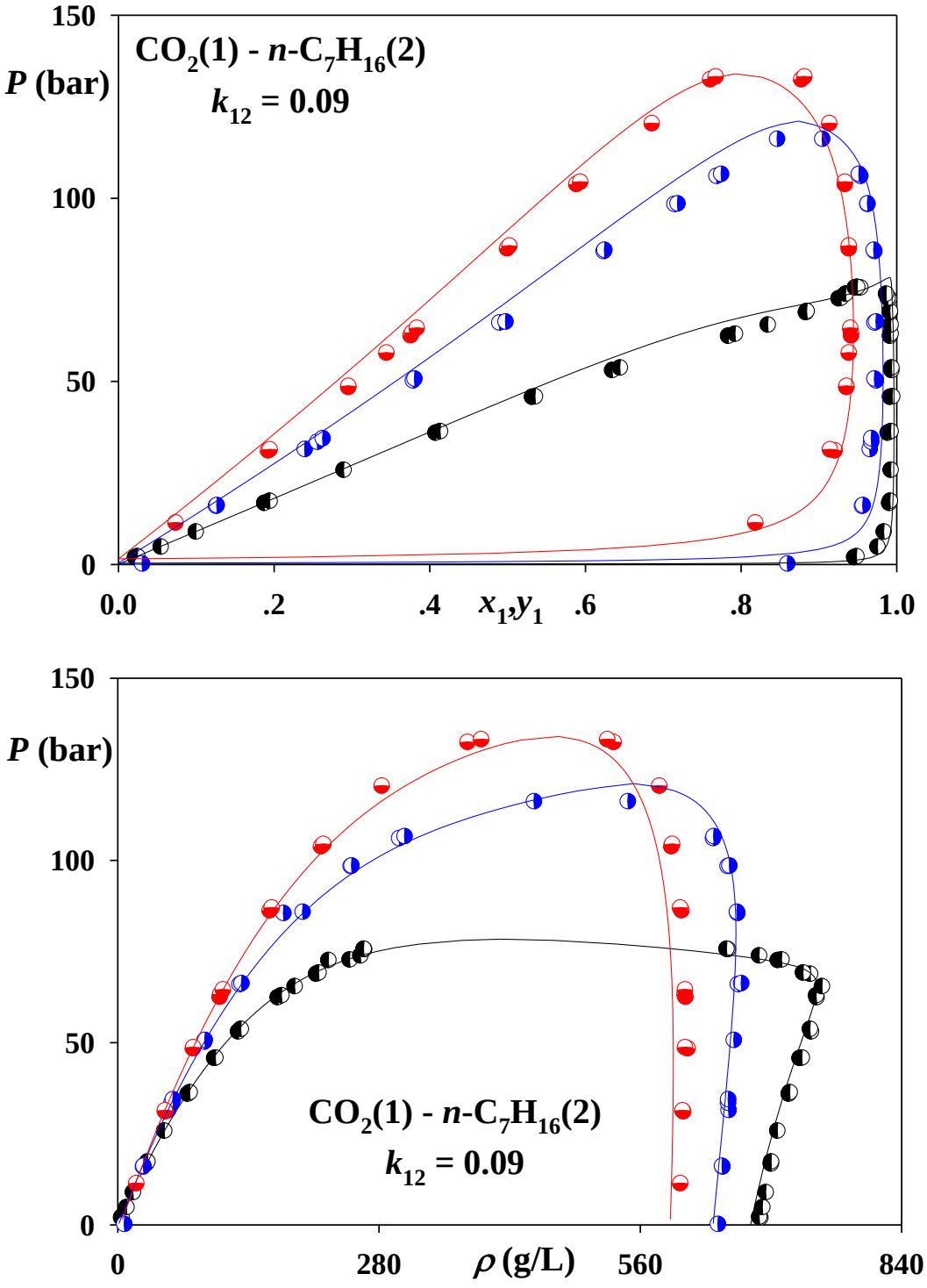

Figure S19. VLE and saturated phase densities of carbon dioxide(1) – *n*-heptane(2). Experimental data[30]: ◑ – 310.37 K, ◐ – 352.59 K, ◓ – 394.26 K. Lines – results of CP-PC-SAFT.

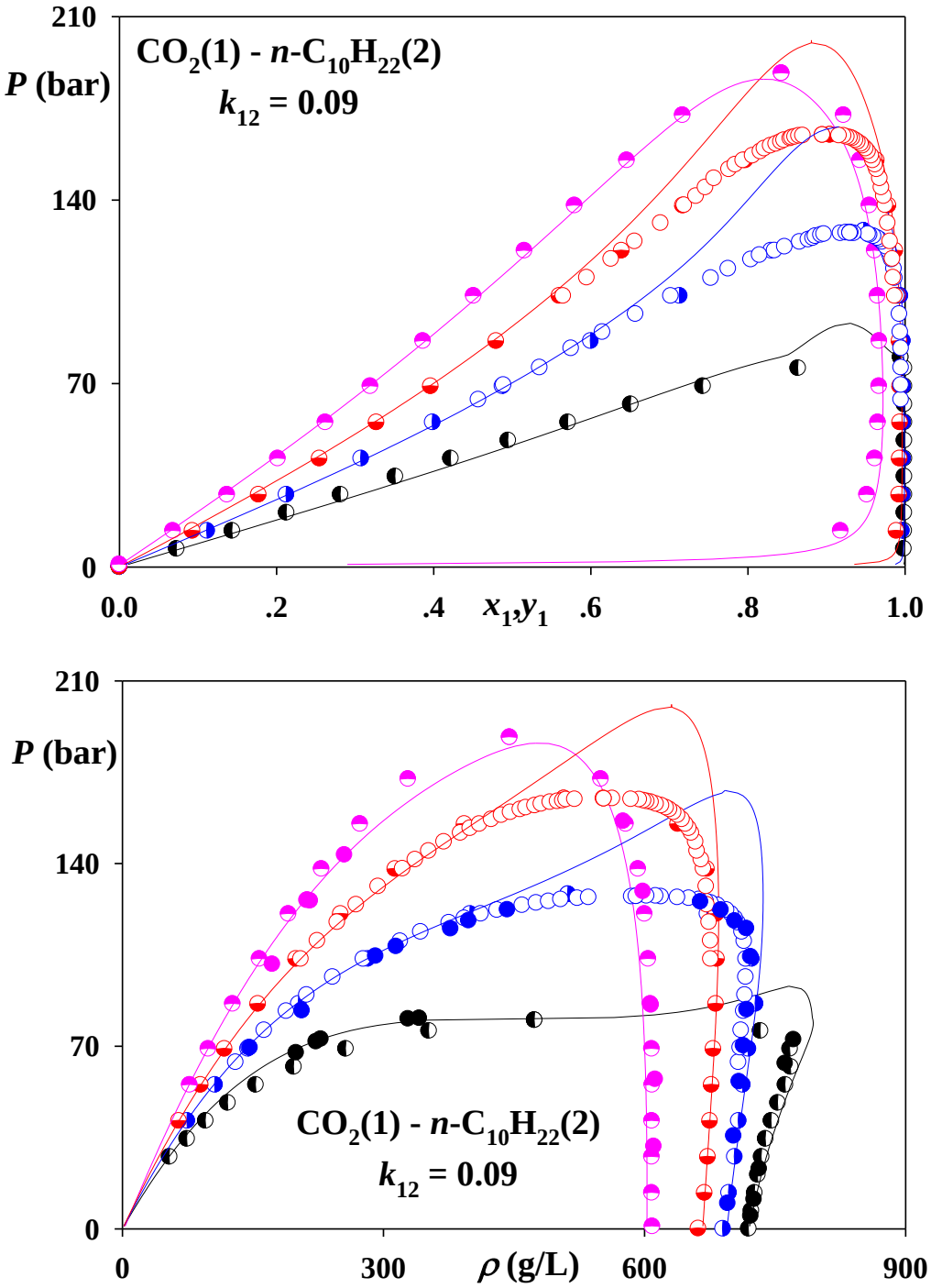

Figure S20. VLE and saturated phase densities of carbon dioxide (1) – *n*-decane(2). Experimental data: ◑ – 310.93 K, ◐ – 344.26 K, ◓ – 377.59 K ◒ – 444.26 K[31]; ○ – 344.3 K, ○ – 377.6 K[32]; ● –313.4 K; ● – 343.3 K, ● – 443.1 K[12]; Lines – results of CP-PC-SAFT.

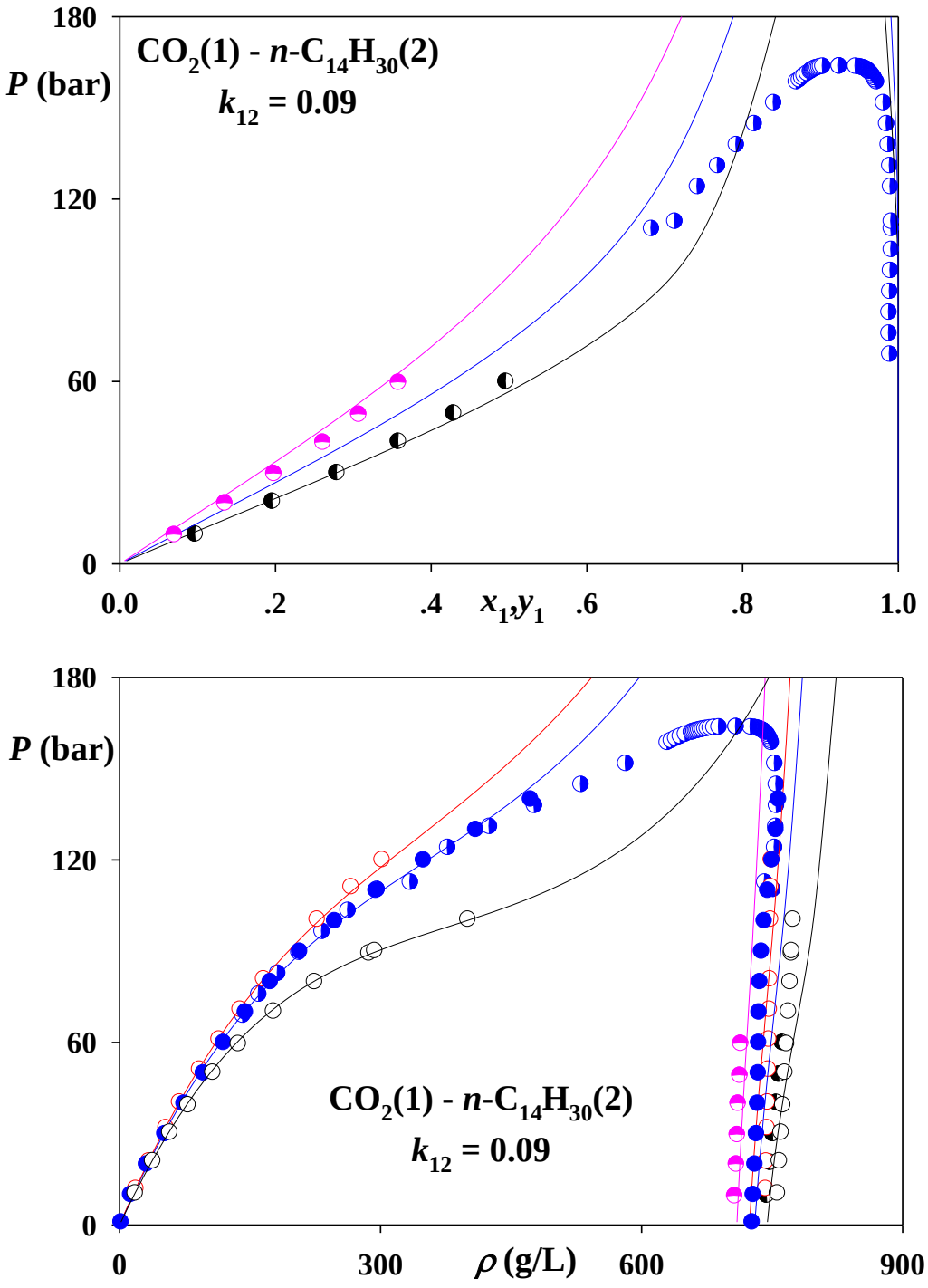

Figure S21. VLE and saturated phase densities of carbon dioxide (1) – *n*-tetradecane(2). Experimental data: ◑ – 323.2 K[33]; ◐ – 344.3 K[34]; ◒ – 373.2 K[35]; ● – 344.15 K[36]; ○ – 323.15 K, ○ – 353.15 K[37]. Lines – results of CP-PC-SAFT.

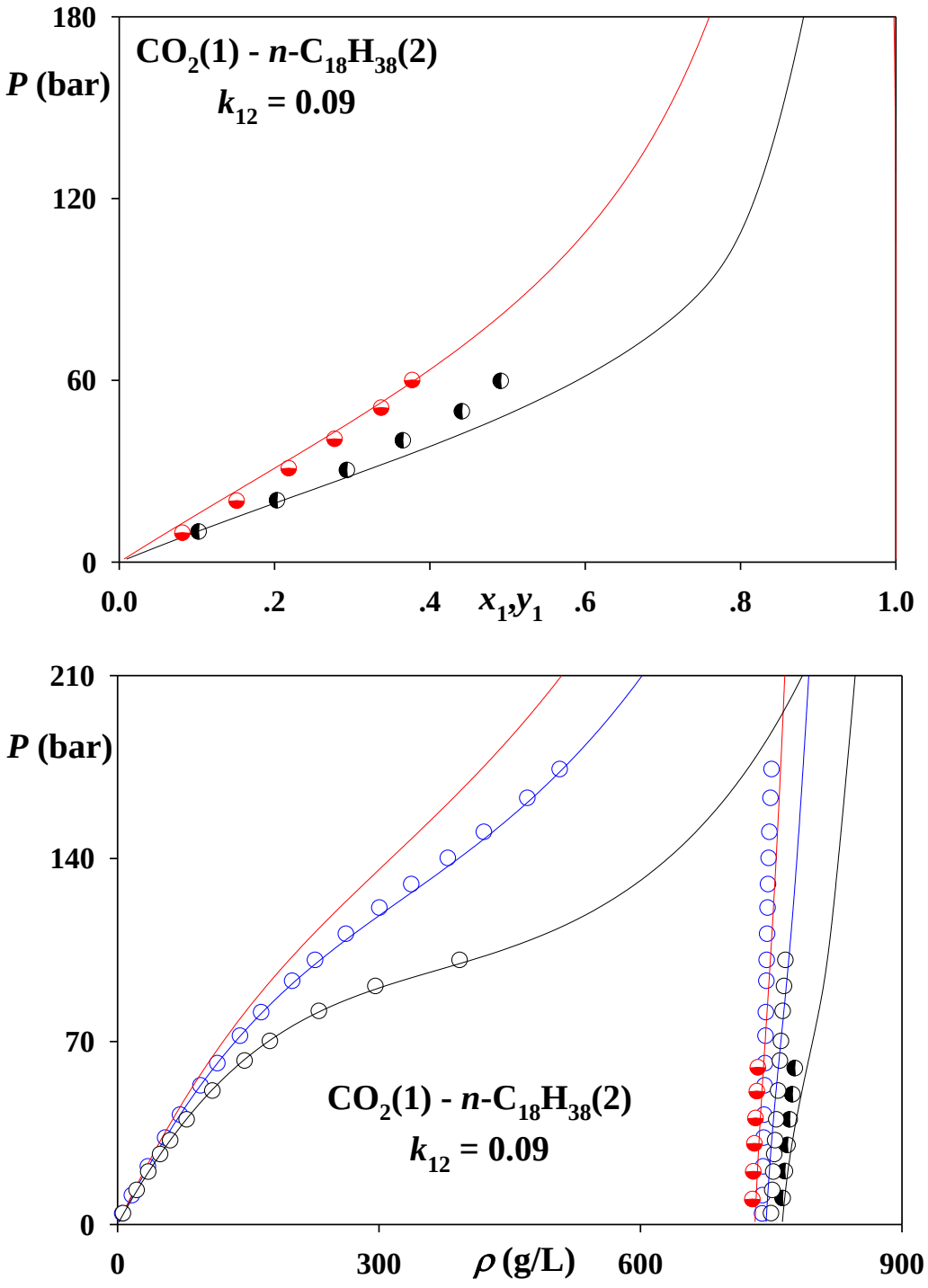

Figure S22. VLE and saturated phase densities of carbon dioxide (1) – *n*-octadecane(2). Experimental data: ◑ – 323.1 K[38]; ◓ – 373.2 K[39]; ○ – 323.15 K, ○ – 353.15 K[37]. Lines – results of CP-PC-SAFT.

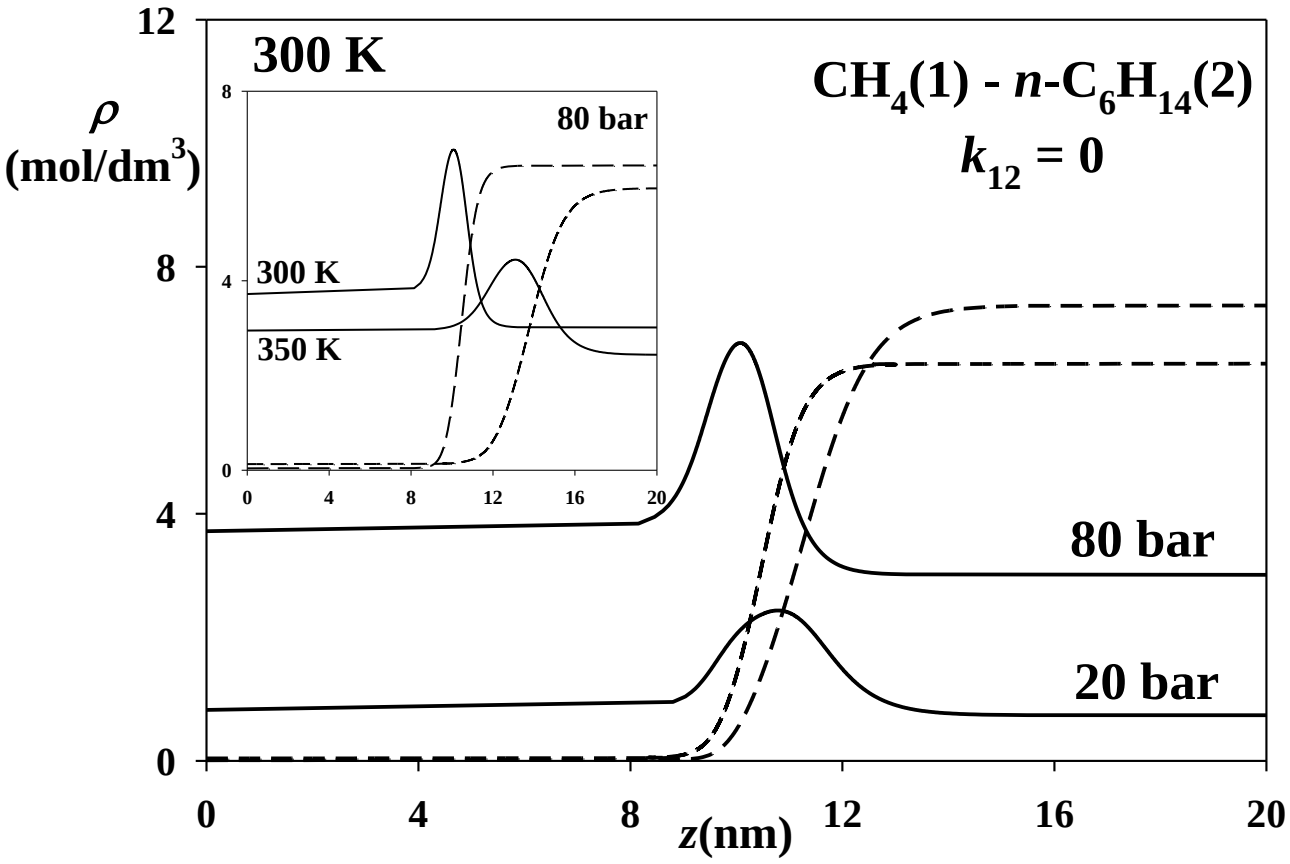

Figure S23. Density profiles of methane(1) – *n*-hexane(2) across the vapor−liquid surface, at T = 300 K and P = 80 bar (inset plot). Solid lines – the results for methane, dashed lines – for *n*-hexane.

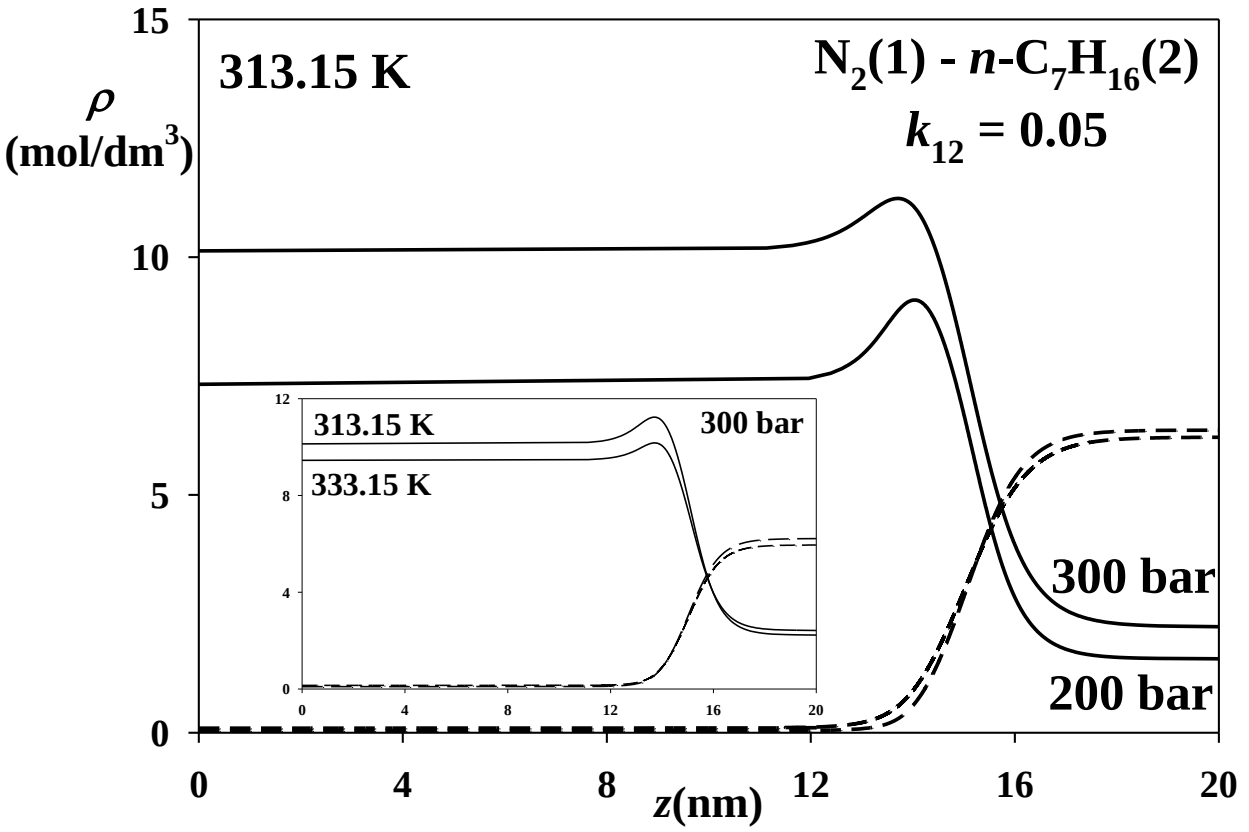

Figure S24. Density profiles of nitrogen(1) – *n*-heptane(2) across the vapor−liquid surface, at T = 313.15 K and P = 300 bar (inset plot). Solid lines – the results for nitrogen, dashed lines – for *n*-heptane

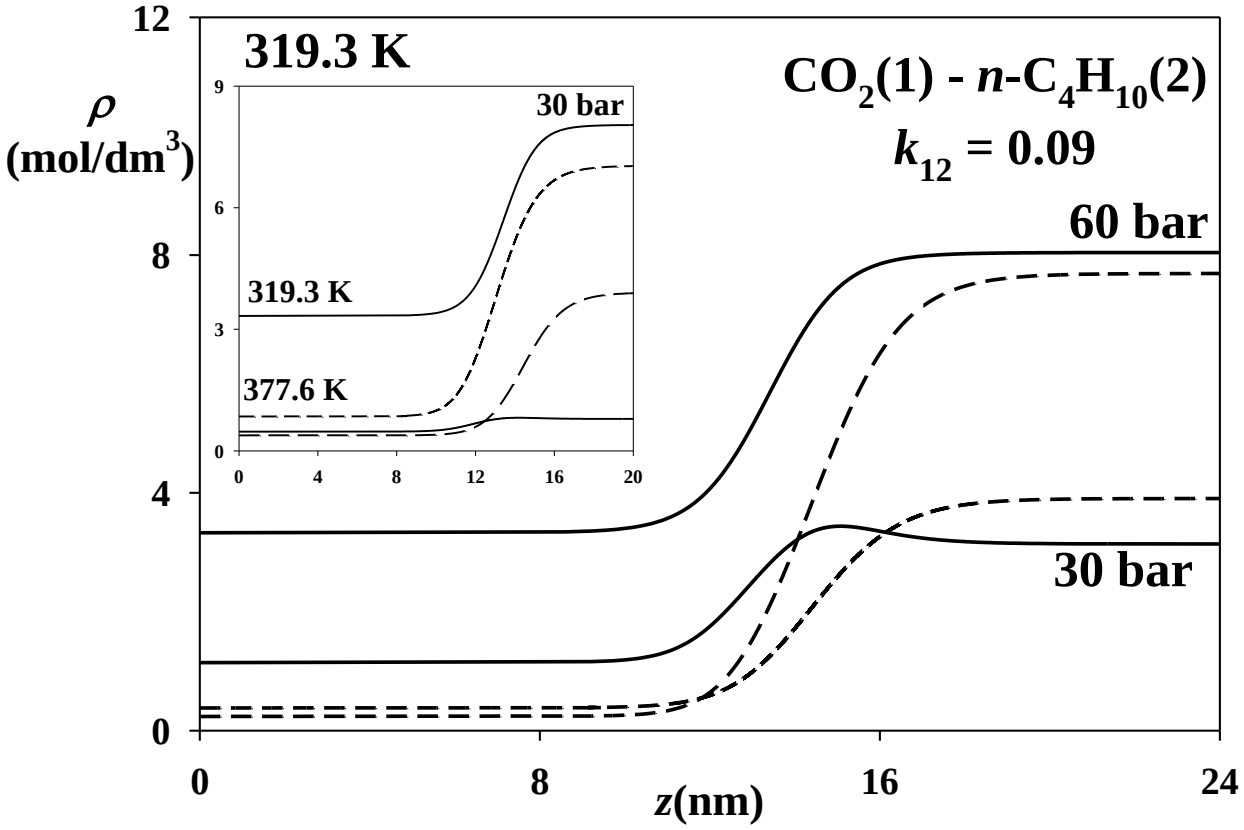

Figure S25. Density profiles of carbon dioxide(1) – *n*-butane(2) across the vapor−liquid surface, at T = 319.3 K and P = 30 bar (inset plot). Solid lines – the results for carbon dioxide, dashed lines – *n*-butane.

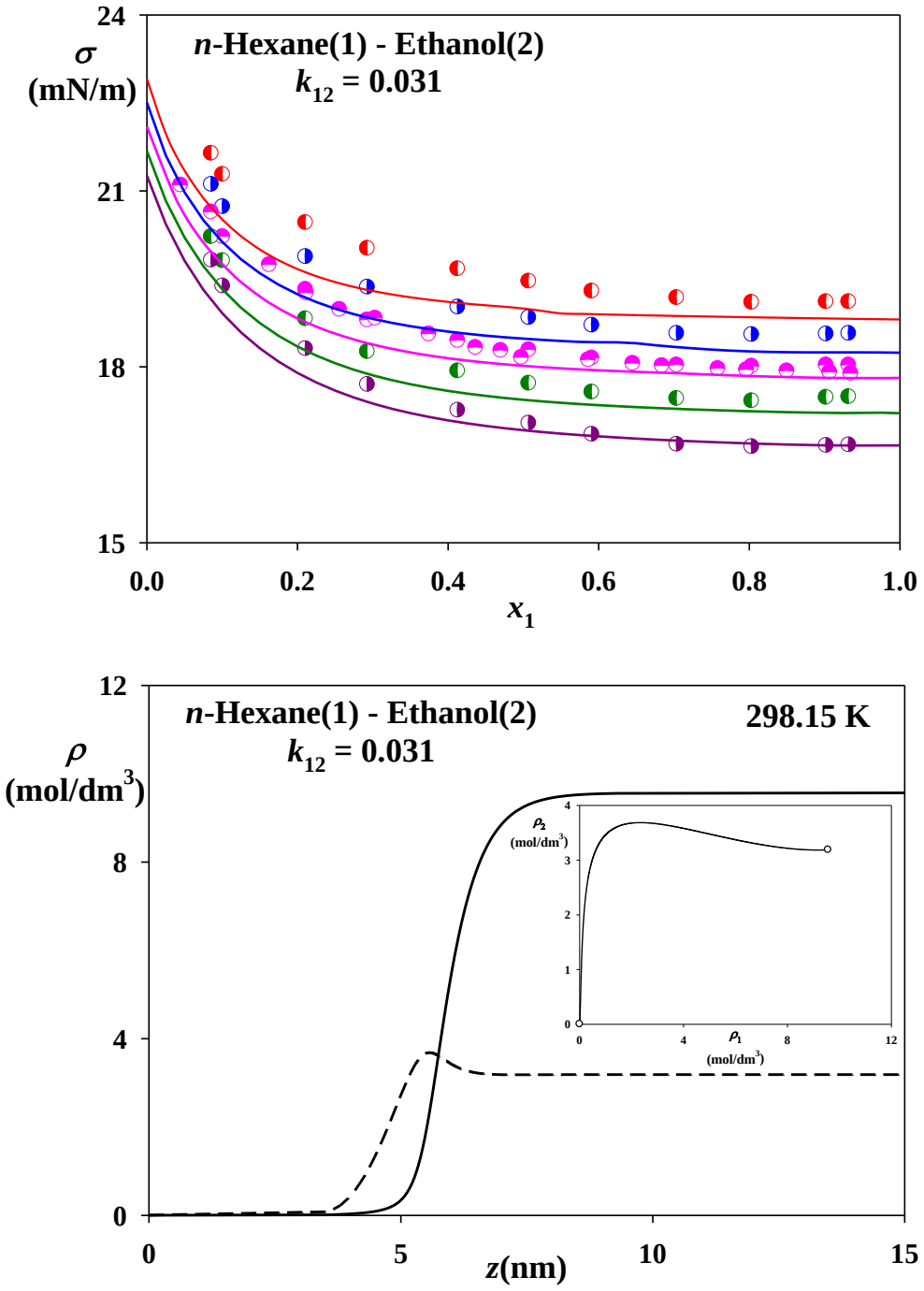

Figure S26. ST and density profiles of *n*-hexane (1) – ethanol(2). Experimental data: ◐ 288.15 K[41] ◑ – 293.15 K[41], ◓ – 298.15 K[40,41] ◐ 303.15 K[41] ◑ – 308.15 K[41]; Lines – predictions of the proposed approach with $k_{12} = 0.031$ and $\beta = 1$.

References

(1) Wiegand, G.; Franck, E. U. Interfacial Tension between Water and Non-Polar Fluids up to 473 K and 2800 bar. *Ber. Bunsenges. Phys. Chem.* **1994**, *98*, 809.

(2) Raabe, G.; Janisch, J.; Koehler J. Experimental Studies of Phase Equilibria in Mixtures Relevant for the Description of Natural Gases. *Fluid Phase Equilib.* **2001**, *185*, 199.

(3) Janisch, J.; Raabe, G.; Köhler, J. Vapor-Liquid Equilibria and Saturated Liquid Densities in Binary Mixtures of Nitrogen, Methane, and Ethane and their Correlation Using the VTPR and PSRK GCEOS. *J. Chem. Eng. Data* **2007**, *52*, 1897.

(4) Reamer, H. H.; Sage, B. H.; Lacey, W. N. Phase Equilibria in Hydrocarbon Systems. Volumetric and Phase Behavior of the Methane-Propane System. *Ind. Eng. Chem.* **1950**, *42*, 534.

(5) Berry, V. M.; Sage, B. H. Phase Behavior in Binary and Multicomponent Systems at Elevated Pressures: *n*-Pentane and Methane-*n*-Pentane. Nat. Stand. Ref. Data Ser. NSRDS-NBS 32, **1970**, https://nvlpubs.nist.gov/nistpubs/Legacy/NSRDS/nbsnsrds32.pdf

(6) Satherley, J.; Cooper, D. L.; Schiffrin, D. J. Surface Tension, Density and Composition in the Methane-Pentane System at High Pressure. *Fluid Phase Equilib*. **2018**, *456*, 193.

(7) Reiff, W. E.; Peters-Gerth, P.; Lucas, K. A Static Equilibrium Apparatus for (Vapour + Liquid) Equilibrium Measurements at High Temperatures and Pressures. Results for (Methane + *n*-Pentane). *J. Chem. Thermodyn.* **1987**, *19*, 467.

(8) Shim, J.; Kohn, J. P. Multiphase and Volumetric Equilibria of Methane – *n*-Hexane Binary System at Temperatures Between –110° and 150 ° C. *J. Chem. Eng. Data* **1962**, *7*, 3.

(9) Marteau, Ph.; Obriot, J; Barreau, A.; Ruffier-Meray, V. Behar E. Experimental Determination of the Phase Behavior of Binary Mixtures: Methane-Hexane and Methane-Benzene. *Fluid Phase Equilib.* **1997**, *129*, 285.

(10) Reamer, H. H.; Sage, B. H.; Lacey, W. N. Volumetric and Phase Behavior of the Methane – *n*-Heptane System. *Ind. Eng. Chem. Chem. Eng. Data. Ser*. **1956**, *1*, 29.

(11) Reamer, H. H.; Olds, R. H.; Sage, B. H.; Lacey, W. N. Phase Equilibria in Hydrocarbon Systems. Methane – Decane System. *Ind. Eng. Chem*. **1942**, *34*, 1526.

(12) Pereira, L. M. C.; Chapoy, A.; Burgass, R.; Tohidi, B. Measurement and Modelling of High Pressure Density and Interfacial Tension of (Gas + *n*-Alkane) Binary Mixtures. *J. Chem. Thermodyn*. **2016**, *97*, 55.

(13) Kidnay, A. J.; Miller, R. C.; Parrish, W. R.; Hiza, M. J. Liquid-Vapour Phase Equilibria in the N_2-CH_4 System from 130 to 180 K. *Cryogencs* **1975**, *15*, 531.

(14) Baidakov, V. G.; Khotienkova, M. N.; Andbaeva, V. N.; Kaverin, A. M. Capillary Constant and Surface Tension of Methane–Nitrogen Solutions: 1. Experiment. *Fluid Phase Equilib*. **2011**, *301*, 67.

(15) Gupta, M. K.; Gardner, G. C.; Hegarty, M. J.; Kidnay, A. J. Liquid-Vapor Equilibria for the N_2 + CH_4 + C_2H_6 System from 260 to 280 K. *J. Chem. Eng. Data* **1980**, *25*, 313.

(16) Kalra, H.; Robinson, D. B.; Besserer, G. J. The Equilibrium Phase Properties of the Nitrogen-*n*-Pentane System. *J. Chem. Eng. Data* **1977**, *22*, 215.

(17) Tang, J.; Satherley, J.; Schiffiin, D. J. Density and Interfacial Tension of Nitrogen-Hydrocarbon Systems at Elevated Pressures. *Chin. J. Chem. Eng*. **1993**, *1*, 223.

(18) Silva-Oliver, G.; Eliosa-Jiménez, G.; García-Sánchez, F.; Avendaño-Gómez, J. R. High-Pressure Vapor–Liquid Equilibria in the Nitrogen–*n*-Pentane System. *Fluid Phase Equilib*. **2006**, *250*, 37.

(19) Poston, R.; McKetta, J. J. Vapor-Liquid Equilibrium in the *n*-Hexane-Nitrogen System. *J. Chem. Eng. Data* **1966**, *11*, 364.

(20) Eliosa-Jiménez, G.; Silva-Oliver, G.; García-Sánchez, F.; de Ita de la Torre, A. High-Pressure Vapor-Liquid Equilibria in the Nitrogen + *n*-Hexane System. *J. Chem. Eng. Data* **2007**, *52*, 395.

(21) García-Sánchez, F.; Eliosa-Jiménez, G.; Silva-Oliver, G.; Godínez-Silva, A. High-Pressure (Vapor + Liquid) Equilibria in the (Nitrogen + *n*-Heptane) System. *J. Chem. Thermodyn*. **2007**, *39*, 893.

(22) Akers, W. W.; Kehn, D. M.; Kilgore, C. H. Volumetric and Phase Behavior of Nitrogen-Hydrocarbon Systems. *Ind. Eng. Chem*. **1954**, *46*, 2536.

(23) Llave, F. M.; Chung, T. H. Vapor-Liquid Equilibria of Nitrogen-Hydrocarbon Systems at Elevated Pressures. *J. Chem. Eng. Data* **1988**, *33*, 123.

(24) Eliosa-Jiménez, G.; García-Sánchez, F.; Silva-Oliver, G.; Macías-Salinas, R. Vapor–Liquid Equilibrium Data for the Nitrogen + *n*-Octane System from (344.5 to 543.5) K and at Pressures up to 50 MPa. *Fluid Phase Equilib*. **2009**, *282*, 3.

(25) García-Sánchez, F.; Eliosa-Jiménez, G.; Silva-Oliver, G.; García-Flores, B. E.; Vapor-Liquid Equilibrium Data for the Nitrogen + *n*-Decane System from (344 to 563) K and at Pressures up to 50 MPa. *J Chem. Eng. Data* **2009**, *54*, 1560.

(26) Sultanov, R. G.; Skripka, V. G.; Namiot, A. Y. Phase Equilibria in the Systems Methane - *n*-Hexadecane and Nitrogen - *n*-Hexadecane at High Temperatures and Pressures. Deposited Doc VINITI **1971** (data obtained from DDB).

(27) Richon, D.; Laugler, S.; Renon, H. High-Pressure Vapor-Liquid Equilibrium Data for Binary Mixtures Containing N_2, CO_2, H_2S, and an Aromatic Hydrocarbon or Propylcyclohexane in the Range 313-473 K. *J Chem. Eng. Data* **1992**, *37*, 264.

(28) Hsu, J. J. C.; Nagarajan, N.; Robinson, Jr, R. L. Equilibrium Phase Compositions, Phase Densities, and Interfacial Tensions for CO_2 + Hydrocarbon Systems. 1. CO_2 + *n*-Butane. *J Chem. Eng. Data* **1985**, *30*, 485.

(29) Besserer, G. J.; Robinson, D. B. Equilibrium-Phase Properties of *n*-Pentane-Carbon Dioxide System. *J Chem. Eng. Data* **1973**, *18*, 416.

(30) Kalra, H.; Kubota, H.; Robinson, D. B.; Ng, H. J. Equilibrium Phase Properties of the Carbon Dioxide-*n*-Heptane System. *J Chem. Eng. Data* **1978**, *23*, 317.

(31) Reamer, H. H.; Sage, B. H. Phase Equilibria in Hydrocarbon Systems. Volumetric and Phase Behavior of the *n*-Decane-CO_2 System. *J Chem. Eng. Data* **1963**, *8*, 508.

(32) Nagarajan, N.; Robinson, Jr., R. L. Equilibrium Phase Compositions, Phase Densities, and Interfacial Tensions for CO_2 + Hydrocarbon Systems. 2. CO_2 + *n*-Decane. *J Chem. Eng. Data* **1986**, *31*, 168.

(33) Kariznovi, M.; Nourozieh, H.; Abedi, J. Phase Composition and Saturated Liquid Properties in Binary and Ternary Systems Containing Carbon Dioxide, *n*-Decane, and *n*-Tetradecane. *J. Chem. Thermodyn*. **2013**, *57*, 189.

(34) Gasem, K. A. M.; Dickson, K. B.; Dulcamara, P. B.; Nagarajan, N,; Robinson, Jr, R. L. Equilibrium Phase Compositions, Phase Densities, and Interfacial Tensions for CO_2 + Hydrocarbon Systems. 5. CO_2 + *n*-Tetradecane. *J Chem. Eng. Data* **1989**, *34*, 191.

(35) Nourozieh, H.; Kariznovi, M.; Abedi, J. Measurement and Correlation of Saturated Liquid Properties and Gas Solubility for Decane, Tetradecane and Their Binary Mixtures Saturated with Carbon Dioxide. *Fluid Phase Equilib*. **2013**, *337*, 246.

(36) Cumicheo, C.; Cartes, M.; Segura, H.; Müller, E. A.; Mejía, A. High-Pressure Densities and Interfacial Tensions of Binary Systems Containing Carbon Dioxide + *n*-Alkanes: (*n*-Dodecane, *n*-Tridecane, *n*-Tetradecane). *Fluid Phase Equilib*. **2014**, *380*, 82.

(37) Li, N.; Zhang, C. W.; Ma, Q. L.; Jiang, L. Y.; Xu, Y. X.; Chen, G. J.; Sun, C. Y.; Yang, L. Y. Interfacial Tension Measurement and Calculation of (Carbon Dioxide + *n*‑Alkane) Binary Mixtures. *J Chem. Eng. Data* **2017**, *62*, 2861.

(38) Nourozieh, H.; Bayestehparvin, B.; Kariznovi, M.; Abedi, J. Equilibrium Properties of (Carbon Dioxide + *n*‑Decane + *n*-Octadecane) Systems: Experiments and Thermodynamic Modeling. *J Chem. Eng. Data* **2013**, *58*, 1236.

(39) Kariznovi, M.; Nourozieh, H.; Abedi, J. Experimental Results and Thermodynamic Investigation of Carbon Dioxide Solubility in Heavy Liquid Hydrocarbons and Corresponding Phase Properties. *Fluid Phase Equilib*. **2013**, *339*, 105.

(40) Jiménez, E.; Casas, H.; Segade, L.; Franjo, C. Surface Tensions, Refractive Indexes and Excess Molar Volumes of Hexane +1-Alkanol Mixtures at 298.15 K. *J. Chem. Eng. Data* **2000**, *45*, 862.

(41) Giner, B.; Villares, A.; Martin, S.; Artigas, H.; Lafuente, C. Study of the Temperature Dependence of Surface Tensions of Some Alkanol + Hexane Mixtures. *J. Chem. Eng. Data* **2007**, *52*, 1904.

"An example of Mathematica® routine for calculating ST in the system methane(1)–n–pentane(2)";

```
"The CP–PC–SAFT EOS";
R = SetPrecision[0.08314472, 60]; Na = SetPrecision[6.0221415 * 10^23, 60];
W1 = SetPrecision[0.2977, 60];
W2 = SetPrecision[0.33163, 60]; W3 = SetPrecision[0.0010477, 60];
a0 = SetPrecision[{0.880823927666, 1.26235042398, –2.88916037036,
    –0.791682734039, 31.4414035626, –67.7739765931, 37.6471023573}, 60];
a1 = SetPrecision[{–0.349731891574, 1.06133747189, –9.92662697237,
    55.1147516007, –158.619888888, 237.469601780, –146.917589624}, 60];
a2 = SetPrecision[{–0.0415741940832, –0.828880456022, 10.6610090572,
    –42.2676046130, 93.3498157944, –119.982855050, 69.3982688833}, 60];
b0 = SetPrecision[{0.724094694, 2.238279186, –4.002584949,
    –21.00357682, 26.85564136, 206.5513384, –355.6023561}, 60];
b1 = SetPrecision[{–0.575549808, 0.699509552, 3.892567339,
    –17.21547165, 192.6722645, –161.8264617, –165.2076935}, 60];
b2 = SetPrecision[{0.097688312, –0.255757498, –9.155856153,
    20.64207597, –38.80443005, 93.62677408, –29.66690559}, 60];
```

$$\epsilon k12 = \sqrt{\epsilon k11\, \epsilon k22}\,;\ \sigma 12 = \frac{\sigma 11 + \sigma 22}{2};\ m12 = \frac{m11 + m22}{2};\ m = x\, m11 + (1 - x)\, m22;$$

$$\sigma = \left(\left(x^2\, m11^2\, \sigma 11^3 + 2\,(1 - x)\, x\, m11\, m22\, \sigma 12^3 + (1 - x)^2\, m22^2\, \sigma 22^3\right) \Big/ \left(m22\,(1 - x) + m11\, x\right)^2\right)^{1/3};$$

$$\epsilon k = \left(\left(x^2\, \epsilon k11\, m11^2\, \sigma 11^3 + 2\,(1 - x)\, x\, \epsilon k12\, m11\, m22\, \sigma 12^3 + (1 - x)^2\, \epsilon k22\, m22^2\, \sigma 22^3\right) \Big/ \left(m22\,(1 - x) + m11\, x\right)^2\right) \Big/ \sigma^3;$$

$$d11 = \sigma 11\, \frac{1 + W1\, T / \epsilon k11}{1 + W2\, T / \epsilon k11 + W3\, (T / \epsilon k11)^2};$$

$$d22 = \sigma 22\, \frac{1 + W1\, T / \epsilon k22}{1 + W2\, T / \epsilon k22 + W3\, (T / \epsilon k22)^2};$$

$$d12 = \sigma 12\, \frac{1 + W1\, T / \epsilon k12}{1 + W2\, T / \epsilon k12 + W3\, (T / \epsilon k12)^2};$$

$$d = \sigma\, \frac{1 + W1\, T / \epsilon k}{1 + W2\, T / \epsilon k + W3\, (T / \epsilon k)^2};$$

$$\eta 0 = \frac{\pi\, Na}{6\, V}\,(x\, m11 + (1 - x)\, m22);$$

$$\eta 1 = \frac{\pi\, Na}{6\, V}\,(x\, m11\, d11 + (1 - x)\, m22\, d22);$$

$$\eta 2 = \frac{\pi\, Na}{6\, V}\,(x\, m11\, d11^2 + (1 - x)\, m22\, d22^2);$$

$$\eta = \frac{\pi\, Na}{6\, V}\,(x\, m11\, d11^3 + (1 - x)\, m22\, d22^3);$$

$$ghs11 = \frac{1}{1 - \eta} + \frac{3\, d11\, \eta 2}{2\,(1 - \eta)^2} + 2\left(\frac{d11}{2}\right)^2 \frac{\eta 2^2}{(1 - \eta)^3};$$

$$ghs22 = \frac{1}{1-\eta} + \frac{3\,d22\,\eta 2}{2\,(1-\eta)^2} + 2\left(\frac{d22}{2}\right)^2 \frac{\eta 2^2}{(1-\eta)^3};$$

$$ghs12 = \frac{1}{1-\eta} + \frac{3\,d12\,\eta 2}{2\,(1-\eta)^2} + 2\left(\frac{d12}{2}\right)^2 \frac{\eta 2^2}{(1-\eta)^3};$$

"Helmholtz Hard-Sphere";

$$Ahs = R\,T\,\frac{m}{\eta 0}\left(\frac{3\,\eta 1\,\eta 2}{(1-\eta)} + \frac{\eta 2^3}{\eta\,(1-\eta)^2} + \left(\frac{\eta 2^3}{\eta^2} - \eta 0\right)\mathrm{Log}[1-\eta]\right)\frac{\sqrt{1-\eta}}{\sqrt{\frac{d^3-\eta\,\sigma^3}{d^3}}};$$

"Helmholtz Chain formation";

$$Achain = R\,T\,\left(x\,(1-m11)\,\mathrm{Log}[ghs11] + (1-x)\,(1-m22)\,\mathrm{Log}[ghs22]\right);$$

"Helmholtz dispersion";

$$M1 = \frac{\epsilon k22\,m22^2\,\sigma 22^3\,(1-x)^2}{T} + \frac{2\,\epsilon k12\,m11\,m22\,\sigma 12^3\,(1-x)\,x}{T} + \frac{\epsilon k11\,m11^2\,\sigma 11^3\,x^2}{T};$$

$$M2 = \frac{\epsilon k22^2\,m22^2\,\sigma 22^3\,(1-x)^2}{T^2} + \frac{2\,\epsilon k12^2\,m11\,m22\,\sigma 12^3\,(1-x)\,x}{T^2} + \frac{\epsilon k11^2\,m11^2\,\sigma 11^3\,x^2}{T^2};$$

$$a = a0 + \frac{m-1}{m}\,a1 + \frac{m-1}{m}\,\frac{m-2}{m}\,a2;$$

$$b = b0 + \frac{m-1}{m}\,b1 + \frac{m-1}{m}\,\frac{m-2}{m}\,b2;$$

$$I1 = \mathrm{Sum}\left[a[[j]] * \eta^{(j-1)}, \{j, 1, 7\}\right];$$

$$I2 = \mathrm{Sum}\left[b[[j]] * \eta^{(j-1)}, \{j, 1, 7\}\right];$$

$$C1 = 1 + m\,\frac{8\,\eta - 2\,\eta^2}{(1-\eta)^4} + (1-m)\,\frac{20\,\eta - 27\,\eta^2 + 12\,\eta^3 - 2\,\eta^4}{\left((1-\eta)\,(2-\eta)\right)^2};$$

$$Adisp = R\,T\,Na\left(-\frac{2\,\pi}{V}\,I1\,M1 - \frac{\pi}{V\,C1}\,m\,I2\,M2\right);$$

"Ideal contribution";

$$Aid = R\,T\,\left((1-x)\,\mathrm{Log}[1-x] + x\,\mathrm{Log}[x]\right) - R\,T\,\mathrm{Log}[V];$$

"Helmholtz residual energy (Ares)";

$$Ares = Ahs + Achain + Adisp;$$

"Helmholtz total energy (Ahtz)";

$$Ahtz = Ares + Aid;$$

$$Ahtz1 = Ahtz\ /.\ \{x \to (1 - 10\text{^}-20)\};$$

$$Ahtz2 = Ahtz\ /.\ \{x \to 10\text{^}-20\};$$

"Derivative properties";

$$Ax = D[Ahtz, x];$$

$$AV = D[Ahtz, V];$$

$$AT = D[Ahtz, T];$$

$$P = -AV;$$

$$Gf = Ahtz - AV\,V;$$

$$Gx = Ax;$$

```
Mu1 = Gf + (1 - x) Gx;
Mu2 = Gf - x Gx;

"Helmholtz total energy (Ha01) for pure fluids";
Ha01 = ((Ahtz1 * rhosgt1) /. {V -> 1/rhosgt1});
CPot1 = D[Ha01, rhosgt1];
Ha02 = ((Ahtz2 * rhosgt2) /. {V -> 1/rhosgt2});
CPot2 = D[Ha02, rhosgt2];

"Objective Function for Phase Equilibria";
fa0 = (P /. {x → (1 - 10^-20), V → Vl1}) - (P /. {x → (1 - 10^-20), V → Vg1});
fa1 = (Gf /. {x → (1 - 10^-20), V → Vl1}) - (Gf /. {x → (1 - 10^-20), V → Vg1});
fb0 = (P /. {x → (10^-20), V → Vl2}) - (P /. {x → (10^-20), V → Vg2});
fb1 = (Gf /. {x → (10^-20), V → Vl2}) - (Gf /. {x → (10^-20), V → Vg2});


"Standarized Numerical Solution for pure fluids (CP-PC-SAFT)";

"Entering the DIPPR data of methane (C1): the critical constants,
   coefficients of vapor pressure, liquid density and ST ";
Tc = SetPrecision[190.564, 60];
Pc = SetPrecision[45.99, 60];
Vcexp = SetPrecision[0.0986, 60];
C1 = 39.205; C2 = -1324.4; C3 = -3.4366; C4 = 3.1019 * 10^(-5); C5 = 2;
D1 = 2.9214;
D2 = 0.28976;
D3 = 190.56;
D4 = 0.28881;
Tmin = 90.69;
Mw = 16.0428;
A1 = 0.036557; A2 = 1.1466;
Tmin1 = Tmin;
Mw1 = Mw;
ρexp = D1 D2^-1-(1-T/D3)^D4;
pexp = (e^(C1+C2/T+C4 T^C5+C3 Log[T]) / 100000);
pexp1 = pexp;
ift = A1 (1 - T / Tc) ^A2;
ift1 = ift /. {T → Tmin1};
PC = P /. {T → Tc, V → VC, x → 1};
DD1 = D[PC, VC]; DD2 = D[PC, {VC, 2}];
VC = VD11 Vcexp;
Ptrial = (P /. {V → 1/ρexp}) /. {T → Tmin, x → 1};
pp = pexp /. {T → Tmin};
res = FindRoot[{DD1 == 0, DD2 == 0, PC == Pc, Ptrial == pp}, {ϵk11, 100}, {σ11, 3.51 * 10^-9},
  {m11, 1}, {VD11, 1159/1000}, MaxIterations → 1500, WorkingPrecision → 58]
ϵk11 = ϵk11 /. res; σ11 = σ11 /. res;
m11 = m11 /. res;
VD11 = VD11 /. res;
Print[{DD1, DD2, (PC - Pc)}];
```

```
Clear[Tc, Pc, Vcexp, Tmin, ρexp, D1, D2, D3, D4, pexp,
  C1, C2, C3, C4, C5, PC, DD1, DD2, VC, Ptrial, pp, ift, A1, A2, res];

"Entering the DIPPR data of pentane (C5): the critical constants,
   coefficients of vapor pressure, liquid density and ST ";
Tc = SetPrecision[469.7, 60];
Pc = SetPrecision[33.7, 60];
Vcexp = SetPrecision[0.313, 60];
C1 = 78.741; C2 = -5420.3; C3 = -8.8253; C4 = 9.6171 * 10^(-6); C5 = 2;
D1 = 0.84947;
D2 = 0.26726;
D3 = 469.7;
D4 = 0.27789;
Tmin = 143.42;
Mw = 72.1503;
A1 = 0.05202; A2 = 1.2041;
Tmin2 = Tmin;
Mw2 = Mw;
ρexp = D1 D2^(-1-(1-T/D3)^D4);
pexp = (e^(C1+C2/T+C4 T^C5+C3 Log[T]) / 100000);
pexp2 = pexp;
ift = A1 (1 - T / Tc)^A2;
ift2 = ift /. {T → Tmin2};
PC = P /. {T → Tc, V → VC, x → 10^-13};
DD1 = D[PC, VC]; DD2 = D[PC, {VC, 2}];
VC = VD22 Vcexp;
Ptrial = (P /. {V → 1 / ρexp}) /. {T → Tmin, x → 10^-13};
pp = pexp /. {T → Tmin};
res = FindRoot[{DD1 == 0, DD2 == 0, PC == Pc, Ptrial == pp}, {ϵk22, 202}, {σ22, 3.6 * 10^-9},
  {m22, 3}, {VD22, 1155 / 1000}, MaxIterations → 1500, WorkingPrecision → 58]
ϵk22 = ϵk22 /. res; σ22 = σ22 /. res;
m22 = m22 /. res;
VD22 = VD22 /. res;
Print[{DD1, DD2, (PC - Pc)}];

"Standarized Numerical Solution for pure influence parameters (SGT+CP-PC-SAFT)";

Vl10 = V /. FindRoot[(P /. {x → 1, T → Tmin1}) == (pexp1 /. {T → Tmin1}),
    {V, (2 * V * η /. {x → 1, T → Tmin1})}, MaxIterations → 150, WorkingPrecision → 55];
Vg10 = V /. FindRoot[(P /. {x → 1, T → Tmin1}) == (pexp1 /. {T → Tmin1}),
    {V, 10^6}, MaxIterations → 150, WorkingPrecision → 55];
Vl02 = V /. FindRoot[(P /. {x → 10^-15, T → Tmin2}) == (pexp2 /. {T → Tmin2}),
    {V, (2 * V * η /. {x → 10^-15, T → Tmin1})},
    MaxIterations → 150, WorkingPrecision → 55];
Vg02 = V /. FindRoot[(P /. {x → 10^-15, T → Tmin2}) == (pexp2 /. {T → Tmin2}),
    {V, 10^6}, MaxIterations → 150, WorkingPrecision → 55];

eq1 = {Vl1, Vg1} /. FindRoot[
    {(fa0 /. {T → Tmin1}) == 0, (fa1 /. {T → Tmin1}) == 0}, {Vl1, Vl10}, {Vg1, Vg10}];
Vl1 = Chop[eq1[[1]]];
Vg1 = Chop[eq1[[2]]];
```

```
CPotev1 = CPot1 /. {rhosgt1 → 1 / Vg1, T → Tmin1};
Peq1 = P /. {x → 1, V → Vg1, T → Tmin1};
Omsgt1 = (Ha01 /. {T → Tmin1}) - rhosgt1 CPotev1;
DOmsgt1 = Omsgt1 + Peq1;
riftc1 = 10^(11/2) Sqrt[2 * 10^-19] NIntegrate[Sqrt[DOmsgt1],
    {rhosgt1, 1 / Vg1, 1 / Vl1}, MinRecursion → 3, MaxRecursion → 100];
c11sgt = 10^-19 (ift1 / riftc1)^2;

eq2 = {Vl2, Vg2} /. FindRoot[
    {(fb0 /. {T → Tmin2}) == 0, (fb1 /. {T → Tmin2}) == 0}, {Vl2, Vl02}, {Vg2, Vg02}];
Vl2 = Chop[eq2[[1]]];
Vg2 = Chop[eq2[[2]]];
CPotev2 = CPot2 /. {rhosgt2 → 1 / Vg2, T → Tmin2};
Peq2 = P /. {x → (10^-20), V → Vg2, T → Tmin2};
Omsgt2 = (Ha02 /. {T → Tmin2}) - rhosgt2 CPotev2;
DOmsgt2 = Omsgt2 + Peq2;
riftc2 = 10^(11/2) Sqrt[2 * 10^-19] NIntegrate[Sqrt[DOmsgt2],
    {rhosgt2, 1 / Vg2, 1 / Vl2}, MinRecursion → 3, MaxRecursion → 100];
c22sgt = 10^-19 (ift2 / riftc2)^2;
"Helmholtz Density energy (Ha0) in Mixtures";

Rho = Rho1 + Rho2;

Ha0 = ((Ahtz * Rho) /. {x -> Rho1/Rho, V -> 1/Rho});
Pa0 = P /. {x -> Rho1/Rho, V -> 1/Rho};

PQ1 = D[Ha0, Rho1];
PQ2 = D[Ha0, Rho2];

"TEST POINT at 70 bar";
tph = {313.15, 70, 0.2, 0.998, 0.10`, 0.32};

T = tph[[1]];
P0 = tph[[2]];
x0 = tph[[3]];
y0 = tph[[4]];
RhoL0 = 1 / tph[[5]];
RhoV0 = 1 / tph[[6]];

f1 = (PQ1 /. {Rho1 → x * RhoL, Rho2 → (1 - x) * RhoL}) -
    (PQ1 /. {Rho1 → y * RhoV, Rho2 → (1 - y) * RhoV});
f2 = (PQ2 /. {Rho1 → x * RhoL, Rho2 → (1 - x) * RhoL}) -
    (PQ2 /. {Rho1 → y * RhoV, Rho2 → (1 - y) * RhoV});
f3 = (Pa0 /. {Rho1 → x * RhoL, Rho2 → (1 - x) * RhoL}) - P0;
f4 = (Pa0 /. {Rho1 → y * RhoV, Rho2 → (1 - y) * RhoV}) - P0;

sol = {RhoL, RhoV, x, y} /. FindRoot[
    {f1 == 0, f2 == 0, f3 == 0, f4 == 0}, {RhoL, RhoL0}, {RhoV, RhoV0}, {x, x0}, {y, y0}];

RoL = Re[sol[[1]]];
RoV = Re[sol[[2]]];
```

```
x = Re[sol[[3]]];
y = Re[sol[[4]]] ;

Rho1L = x * RoL;
Rho2L = (1 - x) * RoL;
Rho1V = y * RoV;
Rho2V = (1 - y) * RoV;

PQ1e = PQ1 /. {Rho1 → Rho1L, Rho2 → Rho2L};
PQ2e = PQ2 /. {Rho1 -> Rho1L, Rho2 → Rho2L};
W = Ha0 - (Rho1 * PQ1e + Rho2 * PQ2e);
Wsat = W /. {Rho1 → Rho1L, Rho2 → Rho2L};

"Solution of SGT (minimum energy condition) in space-density";
beta = 0;
c12sgt = (1 - beta) * Sqrt[c11sgt * c22sgt];
h1 = Rho2V;
h2 = Rho2L;
n = 1000;
h = (h2 - h1) / n ;
valro2 = Table[h1 + j * h, {j, 0, n}];
q = Length[valro2];
ec = Sqrt[c11sgt] * (PQ2 - PQ2e) - Sqrt[c22sgt] * (PQ1 - PQ1e);
Rho10 = Rho1V;
k = 0;
Table[k = k + 1;
  s = {Rho1} /. FindRoot[ec == 0, {Rho1, Rho10}, WorkingPrecision → 10];
  Rho10 = s[[1]];
  val = {Rho2, Rho10};
  kn = Length[val];
  Print[val];
  Table[M_{k,j} = val[[j]], {j, 1, kn}];, {Rho2, valro2}];

matriz = Table[M_{i,j}, {i, 1, k}, {j, 1, kn}];
valro1 = matriz[[All, 2]];
data = Table[{valro2[[i]], valro1[[i]]}, {i, 1, k}];
plot1 = ListLinePlot[data, PlotStyle → Black];
puntov = {{Rho2V, Rho1V}};
puntol = {{Rho2L, Rho1L}};
plotv = ListPlot[puntov, PlotStyle → Red, PlotRange → All];
plotl = ListPlot[puntol, PlotStyle → Blue, PlotRange → All];
Show[plotv, plotl, plot1, PlotRange → All, AxesLabel → {"ρ2", "ρ1"}]
Export[NotebookDirectory[] <> "RhoRho.xls", data];
```

```
"ST calculation from Eq. (5)";
valro11 = valro1;
valro22 = valro2;
poldro = Interpolation[Transpose[Join[{valro22}, {valro11}]]][Rho2];
d1d2 = (D[poldro, Rho2]) /. {Rho2 → valro22};
W = Ha0 - (Rho1 * PQ1e + Rho2 * PQ2e);
den2 = 2 * ((W /. {Rho1 → valro11}) - Wsat);
num2 = (c22sgt + 2 * c12sgt * dro1dro2 + c11sgt * dro1dro2^2) /. {dro1dro2 → d1d2};
g2 = Sqrt[den2 * num2];
mm = Length[valro11];
valtension2 =
  Table[NIntegrate[g2[[i]], {Rho2, valro22[[i]], valro22[[i + 1]]}], {i, 1, mm - 1}];
p2 = Length[valtension2];

stvalue = 1000 Sum[valtension2[[i]], {i, 1, p2}] * 10^(11/2)

"Concentration profiles calculation from Eq. (3)";
datagpt = W /. {Rho1 → valro1, Rho2 → Rho2_i};
Table[der_i = d1d2[[i]], {i, 1, q}];
z_1 = 0;
Table[GPT_i = datagpt[[i]], {i, 1, q}];
valz = -Re[Table[z_(i+1) = Re[z_i] + NIntegrate[
         Sqrt[(1 / (2 * (GPT_i - Wsat))) * (c11sgt * der_i^2 + 2 * c12sgt * der_i + c22sgt))],
         {Rho2_i, valro2[[i + 1]], valro2[[i]]}], {i, 1, q - 1}]];
qq = Length[valz];


dataro11 = Table[valro1[[i]], {i, 2, q}];
datos1 = Table[{valz[[i]], dataro11[[i]]}, {i, 1, qq}];
punto1 = {{z_1, Rho1V}};
dataro1z = Join[punto1, datos1];
dataro22 = Table[valro2[[i]], {i, 2, q}];
datos2 = Table[{valz[[i]], dataro22[[i]]}, {i, 1, qq}];
punto2 = {{z_1, Rho2V}};
dataro2z = Join[punto2, datos2];

plotro1z =
  ListLinePlot[dataro1z, PlotStyle → Black, AxesLabel → {"z", "ρ_1"}, PlotRange → All];
plotro2z = ListLinePlot[dataro2z, PlotStyle → Blue,
    AxesLabel → {"z", "ρ_2"}, PlotRange → All];
Show[plotro1z, plotro2z, PlotRange → All]
Export[NotebookDirectory[] <> "Rho-C1.xls", dataro1z];
Export[NotebookDirectory[] <> "Rho-C5.xls", dataro2z];
```